2015

Synthesis and characterisation of a 3D-printable gelatin – epoxy amine double network hydrogel

Anne Kelly

UNIVERSITY OF WOLLONGONG

Synthesis and characterisation of a 3D-printable gelatin – epoxy amine double network hydrogel

*A thesis submitted in fulfilment of the

requirements for the award of the degree

Maters of Philosophy (Faculty of Science, Medicine & Health)

from

UNIVERSITY OF WOLLONGONG

by

Anne Kelly, BSc. (Hons)

Soft Materials Group, School of Chemistry, Faculty of Science, Medicine and Health

2015

Contents

List of Tables

List of Figures

List of Special Names or Abbreviations

Dp246	Diphenyl(2,4,6-trimethylbenzoyl)phosphine oxide
ED2003	Jeffamine® ED2003
G'	Storage modulus
G"	Loss modulus
G(X%):E(X%)	Percentage of gelatin-methacrylate (G) to ED2003-methacrylate (E) in the total polymer content where X is the listed percentage
GMa	Glycidyl Methacrylate
MA	Methacrylate (referring to either GMa or MAh)
MAh	Methacrylic Anhydride
TPC	Total polymer content
Tx91	Thioxanthen-9-one

Abstract

There is a current need for the development of robust smart materials for a variety of medical, consumer, and manufacturing applications. In addition, these materials require the ability to act as 3D printable inks to undergo rapid prototyping. A UV curable gelatin-epoxy amine double network hydrogel with water content of 80% can be simply produced by a one-pot synthesis. This synthesis method can be performed by methacrylating the individual networks by either a one-step process (simultaneously) or a two-step process (independently). It was found that the two-step process is more effective in producing a mechanically robust material, capable of exhibiting a compressive stress at failure of 2.5 ±0.2 MPa. Significantly, a new 3D printing method has been developed to allow the material to be cured post printing resulting in no significant loss in mechanical strength compared to gels prepared by casting. This method uses the entanglement of gelatin (below 37°C) to give support to the individual printed layers of the structure eliminating the need for UV curing after each layer is printed. Post printing, the structure can be UV cured to increase the mechanical strength of the material to that of the hydrogels prepared by casting. It is envisage that this new printing method in conjunction with new hydrogel chemistries can be utilised to fabricated new materials for applications ranging from biomedical devices to soft robotics.

Acknowledgments

I would like to thank the following people for their endless time, stimulating discussions, technical guidance, and personal support throughout this project; Professor Marc in het Panhuis, Professor Paul Calvert, Dr Holly Warren, Reece Gately, Shannon Bakarich, Dr Patricia Hayes, Alex Keller, Dr Damian Kirchmajer, and Rodney Quiggin (because he's a champ).

1. Introduction

Material Science has grown substantially as a scientific field in the last century. This is due to the need for the development of new materials with specific characteristics or properties to support advancing scientific and manufacturing technologies. Applications in medicine[1], consumer manufacturing[2], and computer technology[3], among others require custom designed materials that are easily producible in order to turn modern concepts into working applications.

To suit these various needs, smart materials have been developed that have the ability to vary their properties through external stimuli. Hydrogels can be considered smart materials due to their swelling ability, biodegradability, and the large variety of natural and synthetic hydrogel polymers with varying qualities that are now available to produce these materials.[4]

Some of the most investigated uses of hydrogel are in medical applications. However, there are also a variety of prominent non-medical applications such as pH meters[5], soft robotics[6], loud speakers[7], fire extinguishers[8,9], agriculture release devices[10], and hydrogel based solar cells[11].

The advantages of hydrogel materials which make them suitable for these application include their similarity to the properties of natural tissue[12–14], their reactivity to variable environments, their high degree of flexibility, and their biocompatible.

These characteristics differ in prominence between natural and synthetic hydrogel networks. Natural hydrogels are commonly known for their biodegradability and biocompatibility. As synthetic hydrogels are artificially manufactured they can be designed with specific characteristics. Most hydrogels used in industry today show an evident lack of mechanical robustness; e.g. contact lens, wound dressings, drug delivery and hygiene products.[15] Although some recent research[16–18] has

shown development in the mechanical robustness of synthetic hydrogels, there is still a need for further development in this field.

Further to this, the structural design complexity, the addition of electrical or fibre components, or the need to incorporate multiple materials into a device, are some of the challenges that can make hydrogel based devices difficult to manufacture.[19] Therefore an important part of the developmental process of smart materials is the research into new fabrication techniques.
Rapid Prototyping is a manufacturing technique that allows for the efficient fabrication of complex devices that may require a variety of components or materials.[20] Examples of rapid prototyping methods include, fused deposition modelling, stereolithography, laminated object manufacturing, inkjet systems, selective laser sintering, and extrusion printing.[21–23] These are already widely used in the manufacturing industry, and have the potential to expand.[24] Research has shown that hydrogels can be easily designed using these techniques.[25–28]

1.1. Hydrogels

Hydrogels are crosslinked polymer networks with hydrophilic properties. This class of materials include members which have a water storage capacity of over 99% due in part to hydrophilic functional groups present on the polymer backbone. These groups attract the negative dipole on water molecules, which are then confined by crosslinking of the polymer networks.[29] The polymer networks working in these systems can be either natural or synthetic chains, and can be crosslinked by either covalent or ionic bonding.

Hydrogels properties can vary depending on the monomer selection, the conditions of synthesis, the degree of swelling, the crosslink density, or changes in stimuli including temperature, pH, and salt concentration.[30–33]

1.1.1. Natural and synthetic hydrogel forming polymers

Natural forming polymers are produced and extracted from nature. Examples include natural rubber, starch, collagen, silk, cellulose, gelatin, gellan gum, proteins, and alginate. The advantage of these polymers is that they can be biocompatible and biodegradable because they are derived from natural materials. However, these polymers often have low mechanical robustness and have slight batch variation due to their natural origin.

Synthetic polymers are derived from petroleum oil and are manufactured in a laboratory setting. Examples include poly(ethylene glycol), poly(vinyl alcohol), polyester, rubber, and nylon. The benefits of synthetic polymers is that can be manufactured with a specific property in mind. As the properties of the polymer are dependent on their structure, being able to design and manipulate a polymers backbone, chain length, or functional groups allows for the design of polymers with specific purposes.[33–37] Although, synthetic polymers are often thought to produce weak hydrogel systems, recent research shows that this is not the case.[16]

1.1.2. Structure

The properties of a hydrogel greatly depend on the polymer chain length within its individual networks. Chain length can effect both the melting point and robustness of a hydrogel.[38,39] Longer chains are more inclined to lead to entanglement. More energy is required to separate these entangled chains. Entanglement also decreases the mobility of the chains which then requires more energy to reorganise. This increase in energy makes it more difficult to break the structural integrity of the material hence increases the robustness of the material.

The robustness of a hydrogel is also influenced by the polymer's degree of branching, where a side chain or functional group is attached to the backbone of a polymer.[38,40] Increased branching causes further entanglement which in turn strengthens the hydrogel. The addition of reactive functional groups can also increase the bonding prospects of the polymer.[41] An example of this can be seen by the contrasting properties of high and low density polyethylene. However, the flexibility of both the backbone and branching must be taken into account. This flexibility will influence the access that functional groups have to generate a chemical cross-link.[42]

1.1.3. Crosslinking

Crosslinking is the process whereby polymer chains are physically or chemically linked without further polymerisation. This linking restricts any chain movement and creates a polymer network structure with viscoelastic properties.

Physical crosslinking is a reversible process that occurs either by polymer chain entanglement, crystallisation, or hydrogen bonding within the polymer structure. It is affected by the temperature of the hydrogels environment and is usually formed by cooling the gel.

Chemical crosslinking occurs due to covalent or ionic bonding between polymer chains. Covalent crosslinking occurs either through a direct link or the use of a crosslinking reagent. This process is irreversible and creates hydrogels that cannot be reshaped once they have been linked.

Crosslinking reagents used in the chemical crosslinking process are bifunctional molecules, i.e. two reactive groups within their structure. This allows for covalent bonding with two different polymers or with one polymer and a crosslinking reagent. The reagents can be homobifunctional, where the

reactive groups are the same, or hetrobifunctional, where the reactive groups are different, allowing for crosslinking with two different functional groups.[43]

Additionally, either of the above mentioned bifunctional groups can be photoreactive crosslinking reagents. When exposed to high intensity UV rays in the presents of a curing agent, a photochemical reaction takes place to polymerise the monomers while creating chemical crosslinks between the chains and hence cure the hydrogel.[44,45] Methacrylic anhydride (MAh) and glycidyl methacrylate (GMa) are the two photoreactive crosslinking reagents used in this study, and their structures can be seen in Fig 1.1.

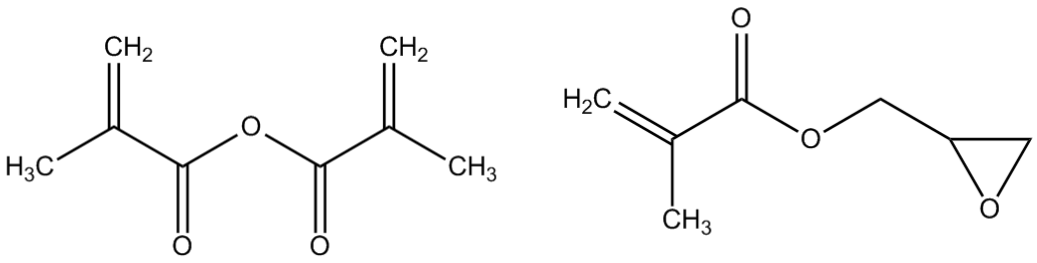

(a) **(b)**

Figure 1.1: Molecular structure of (a) methacrylic anhydride and (b) glycidyl methacrylate

Methacrylic anhydride reacts with water, breaking its central oxygen bond to from methacrylic acid. This reaction must be taken into account when analysing the structural development of the hydrogels throughout this study.

When a photoreactive crosslinking reagent is present, a photoinitiator is added to the solution to initiate the reaction in the presence of UV light. Examples of photoinitiators can be seen in Fig 1.2.

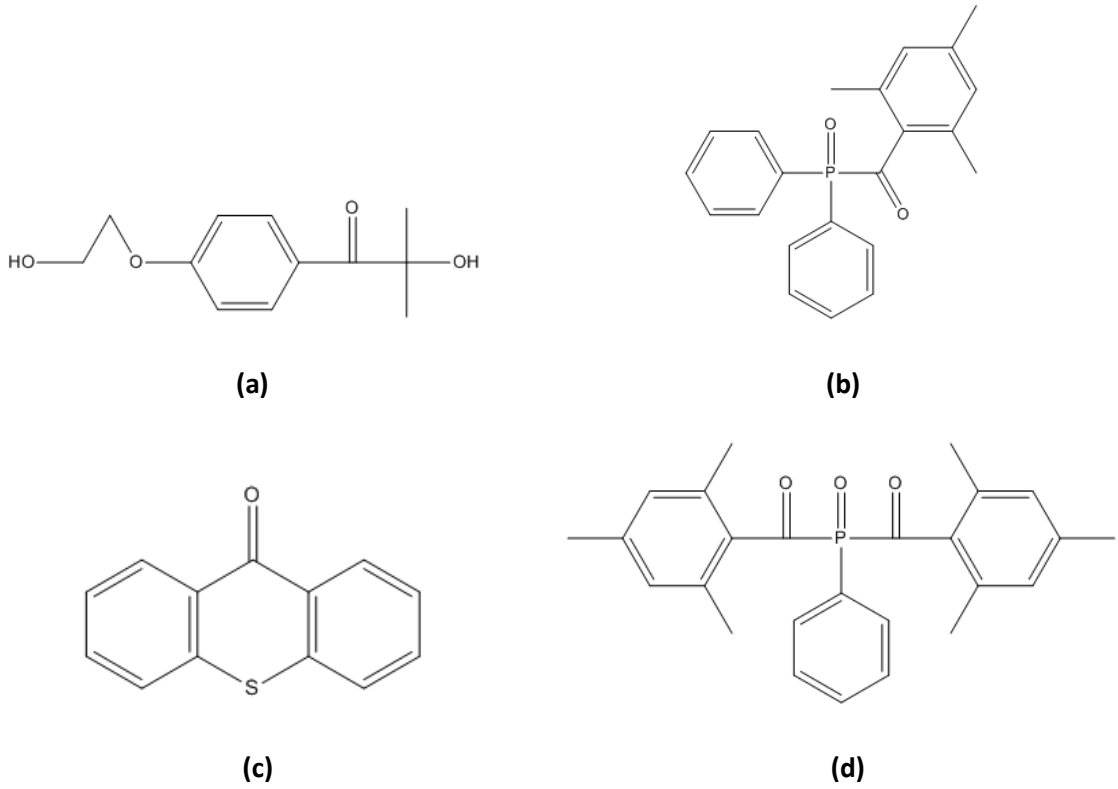

Figure 1.2: Examples of photoinitiators (a) Irgacure 2959 (b) Diphenyl(2,4,6-trimethylbenzoyl)phosphine oxide (c) Thioxanthen-9-one (d) Irgacure 819

This can take place either through abstraction or cleavage of the initiator. When choosing a photoinitiator, the Beer-Lambert law must be taken into account, where the absorption rate of the required wavelength and the extinction coefficient of the initiator are related as follows:

$$A = e\ l\ c, \tag{1}$$

where *A* is the absorbance of the sample, e is the molar absorptivity or extinction coefficient, *c* is the concentration of the solution and *l* is the distance the light passes through. As the extinction coefficient is the measurement of the chemical light absorption, a photoinitiator with a high extinction coefficient will reduce the curing time of the hydrogel.[46]

1.1.4. Swelling

Unlike many other materials that dissolve in water, hydrogels absorb and contain water as a result of a difference in osmotic pressure. The degree of swelling depends on the charge densities of the polymer backbone, the network density, and the cross-link of the networks.[47–50]

As water flows into the hydrogel, negative charges on the polymer backbone attract polar water molecules. The osmotic pressure difference between the hydrogel and the surrounding solution will eventually come to an equilibrium position. At this equilibrium point, a hydrogel with low network and cross-link density will fail to contain the water and hence deform the hydrogel structure. However, a high density crosslinked hydrogel will create an elaborate matrix structure to hold the hydrogel shape in its swollen state. It is well-known that the degree of swelling is dependent on the cross-link density.[31,33]

So far the monomer choice, structure, cross-link ability, and swelling of single network conventional hydrogels have been discussed. Below are some examples of how these operatives can be used to different effects by combining multiple polymer networks.

1.1.5. Hydrogels with two polymer networks

Conventional, and more specifically, synthetic hydrogels have poor mechanical robustness, but it has been shown that combining two polymer networks can produce a more robust hydrogel product than either of the individual polymer networks alone.[51–53] As there are two networks involved, these hydrogels have a higher molecular mass than either individual system, which are used to provide additional support in increasing the mechanical properties of a hydrogel.[54] Below are some examples of hydrogels with two polymer networks.

Interpenetrating Networks (IPN)

Interpenetrating Networks consist of two polymer networks entangled on a molecular level which are not covalently bonded but cannot be separated unless a chemical bond is broken. Combining two networks produces reinforced hydrogels with a broader range of properties and robustness. [53,55] Two of the most common types of IPN hydrogels are Double Network hydrogels and Ionic-Covalent Entanglement hydrogels.

Double Networks (DN)

The structural development of Double Networks hydrogels relies on using two contrasting polymer networks to support each other giving the hydrogel an increased robustness. For example, combining short chain, brittle polymers (minor first network) with long chain, elastic polymers (major second network).[52] As the brittle polymer chain breaks, it disperses mechanical energy over a larger area, the ductile polymer absorbs this damage using its elastic properties. The disadvantage of this system is that the first network is irreparable so the systems cannot be recovered.[16,17,52,56]

Ionic-Covalent Entanglement (ICE)

Ionic-Covalent Entanglement hydrogels are comprised of one covalently bonded polymer network and one ionically bonded polymer network to form an IPN hydrogel structure. ICE hydrogels work on the same bases as a DN gel, however, as the first network is ionically bonded, these bonds can reform giving the hydrogel a high degree of recoverability.[27,28,51,57]

However different the properties, structures, and developmental methods of hydrogels appear to be, the fundamental development process that all gels undergo is the same: the sol-gel transition.

1.1.6. The sol-gel transition

The sol-gel transition involves the shift of a polymer solution, into a hydrogel with both liquid and solid components; i.e. the transition from a liquid state to a gel state (Fig 1.3).[58] In the liquid state dispersed molecules can move freely. In the gel state they have bonded together to form a network. The network is responsible for the visco-elastic behaviour. [58,59] In order for the sol-gel transition to occur, there must have a minimum particle density in solution.

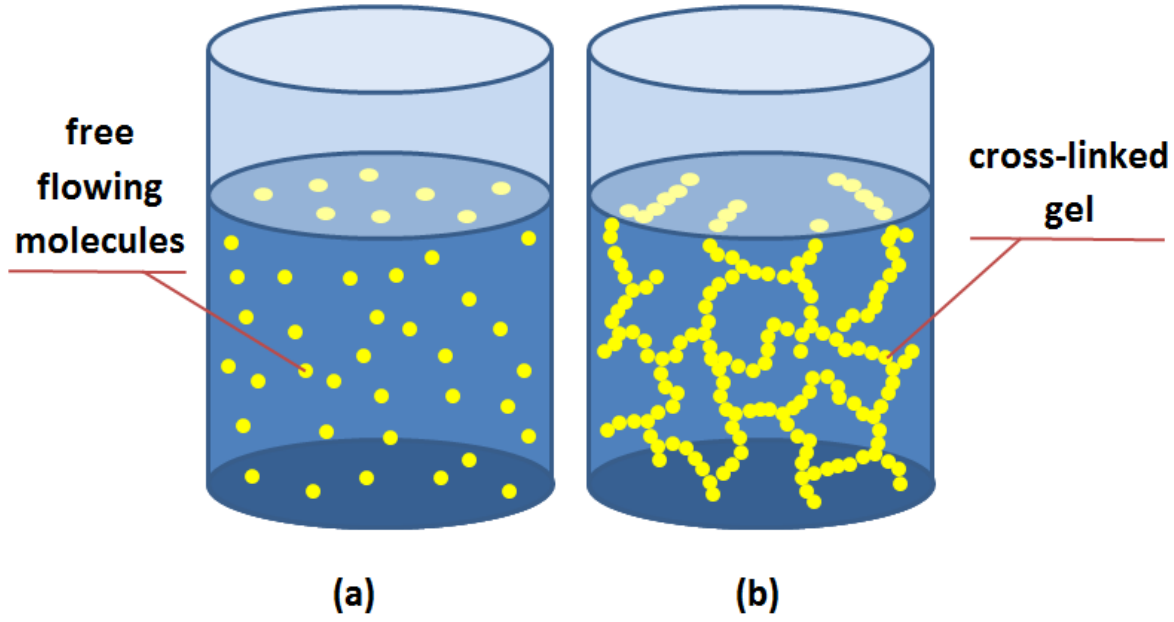

Figure 1.3: An example of the sol-gel transition of a gel where (a) is the liquid state and (b) is the gel state.

1.2. Gelatin

Gelatin is a natural biopolymer derived from the hydrolysis of collagen extracted from animals. Type A gelatin is produced from acid cured proteins while Type B is produced from alkaline cured proteins.[60,61] Type A is commonly used as it is widely available at a low cost and is an optically transparent substance, which is advantageous for UV curing.[60] Gelatin is a common food (e.g. aeroplane jelly) and is US Food and Drug Administration approved.[62]

Gelatin is a multifunctional molecule with extensive branching, which allows it to produce a single network hydrogel that is biodegradable and biocompatible.[63] Gelatin has up to 20 distinctive amino acids with approximately one third of its structure being made from glycine. The remaining structure is approximately 21% proline and hydroxyproline, 10 % Ala, and 36 % other amino acids. The structural pattern of the amino chain typically takes the form –(Gly-X-Y)- where Y is either proline or hydroxyproline, as seen in Fig 1.4, and X is one of the other various amino acids.[64]

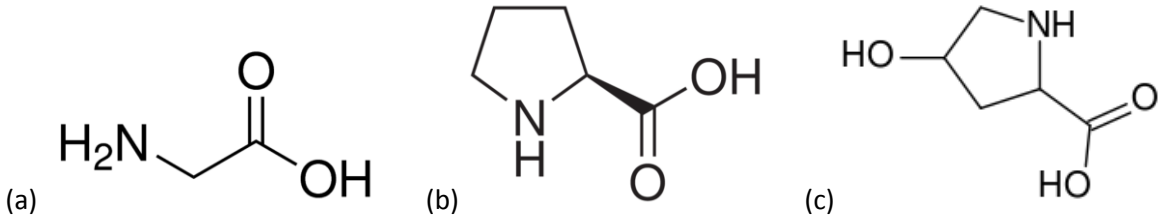

Figure 1.4: Various parts in the structure of gelatin. (a) glycine (b) proline (c) hydroxyproline

Crosslinking and entanglement is an effective way of increasing the robustness of gelatin hydrogels. When dissolved, gelatin will entangle below 35-40 °C. This process is reversible when the temperature is increased above this temperature. Gelatin can also undergo chemical crosslinking through its multiple amine and carboxyl functional groups along its backbone (Fig 1.5).[65]

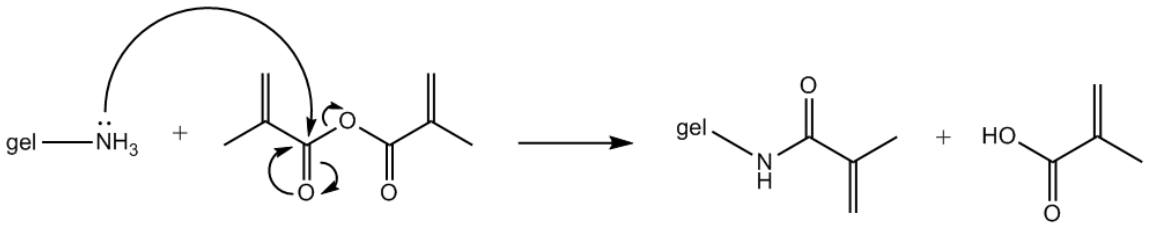

Figure 1.5: An example of the use of gelatines amine functional group.

Gelatin can also undergo crosslinking by photoinitiation when reacted with methacrylates.[66–69] The storage modulus of crosslinked gelatin has been shown to increase compared with simple entanglement of the chains.[70]

Gelatin is already widely used in the manufacturing industry with applications in drug delivery[71], wound dressings[72], glues[73], and sealants[74].

1.3. Jeffamine® ED2003

Jeffamine® ED2003 (hereafter referred to as ED2003) is an aliphatic polyether diamine with a molecular weight of approximately 2000 g/mol. It is a waxy solid at room temperature with a melting point of 43 °C. Structurally, this molecule is a synthetic polymer with two primary amino groups (Fig 1.6). The amino groups are attached at either end of a polyether backbone mainly composed of polyethylene glycol with smaller sections of propylene oxide. The polyethylene glycol allows for complete water solubility.

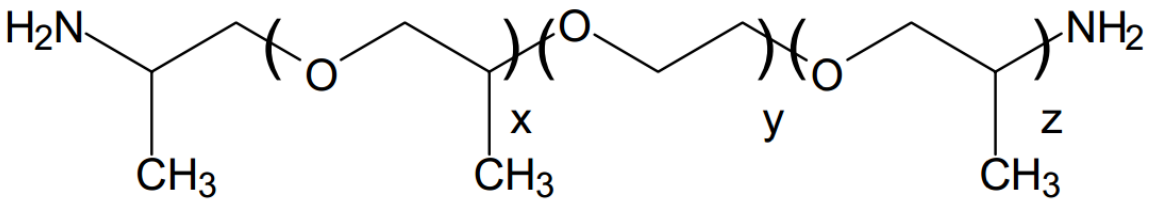

Figure 1.6: Structure of Jeffamine® ED-2003. On average, y = ~39 and x + z = ~6

ED2003 has two functional groups which are both amines meaning it primarily undergoes amine reactions. Jeffamine® products can use these functional groups to undergo a variety of reactions;

epoxy reactions, polyurea linkage, Michael addition, substituted ureas, amide formation, and imine formation.[75]

Although photo curing of Jeffamine® products has been studied[76], no research has been found to specifically produce photo curable ED2003 as an individual product.
Huntsman International LLC produce a wide variety of Jeffamine® products which are often used in composites, castings, decretive and protective coatings due to their transparency, low viscosity, and flexible backbone.[77] These are often used in epoxy modifiers, hydrophilic polymers, and anti-static agents due to their solubility, reactivity, colour, and vapour pressure.[78]

1.4. Methods of synthesis

As previously discussed, one major group of hydrogel forming polymers are produced synthetically. Synthesis processes may be both physical and chemical, and involve multiple steps. Depending on the type of synthesis required, these reactions may take place in one or more reactors. Physical synthesis of hydrogels typically involves cooling and entangling of the polymer chains, where entanglement is the main component locking the chains in place. Chemical synthesis of hydrogels can involves ionic or covalent crosslinking of polymer chains, where bonding is used to hold the chains together.

Both forms of synthesis take place in reactors. Two-pot synthesis uses two different reactors for individual reactions. The products of one reaction is combined with the second network either through further reactions or by mixing to achieve the final outcome (Fig 1.7). An example of two-pot synthesis can be seen in the research done by *Gong, J. P et al* on the production of Double Network hydrogels.[56] One-pot synthesis is a more time efficient method of reacting chemicals. It involves multiple reactions taking place in the same reactor either simultaneously or successively (Fig 1.8). An

example of one-pot synthesis can be seen in research done by *Bakarich, S et al* in the production Ionic-Covalent Entanglement hydrogels.[51]

Although one-pot synthesis can be more time efficient, there is often less control over the reactions taking place. If the reactants are multifunctional, they may be capable of various reactions which can lead to a variety of products. In this case it may be necessary to force specific reactions by separating out the synthesis method into multiple steps.

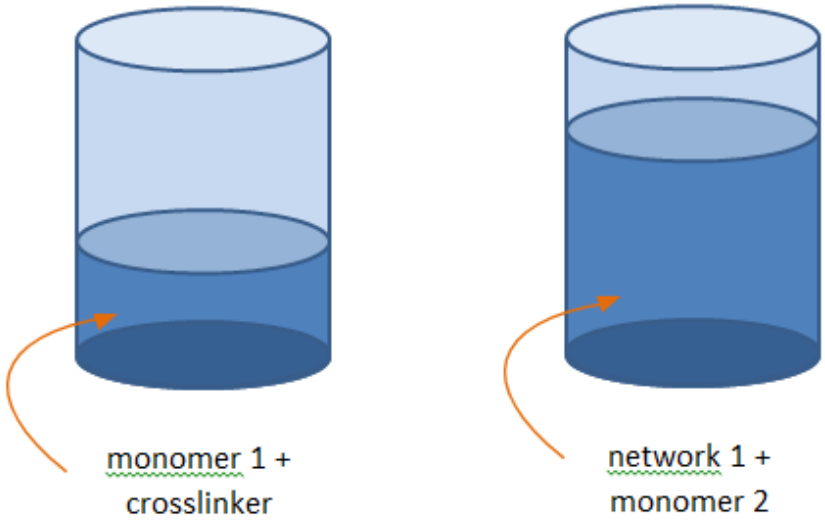

Figure 1.7: An example of two-pot synthesis of a double network hydrogel where (a) is the synthesis of the first network and (b) shows the soaking of the first network in the second monomer leading to polymerisation.

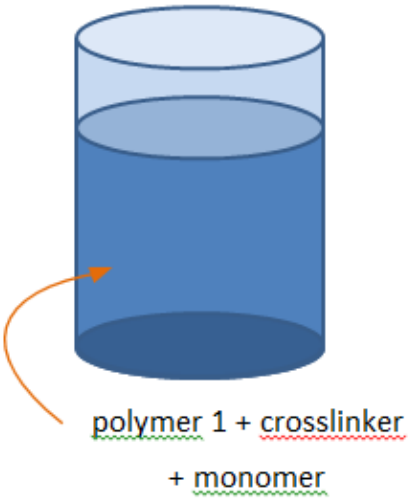

Figure 1.8: *An example of one-pot synthesis of a double network hydrogel where both networks are added to the same vessel before polymerisation.*

1.5. Characterisation Techniques

Tuneable characteristics and robust mechanical properties are two of the main desired qualities of a hydrogel. It is important to be able to assess mechanical and swelling properties for identifying appropriate applications for each hydrogel. There are many techniques to characterise the mechanical robustness of a hydrogel. In this study, the mechanical characteristics are assessed under shear (rheology), under compression (compression testing), and under extension (tensile testing).

1.5.1. Spectroscopy

Fourier transform infrared (FTIR) spectroscopy is a widely used and studied technique to identify the structure of a molecule. Infrared radiation is passed through a sample and some of this energy will be absorbed by the molecular bonds in the sample while the rest will pass through without being affected. The result will produce a spectrum of wavelengths displaying peaks where the signal has been absorbed by the bonds. As different atoms and bonds produce peaks at different wavelengths,

this can be used to determine the various functional groups of the molecules. The additional benefit of using this method is that the height of the peaks are proportional to the number of absorbing units within the volume element sampled. By calculating the ratios of the peak heights is it possible to obtain information about the abundance of each bond within the molecule.

Nuclear magnetic resonance (NMR) spectroscopy is another technique used to determine the structure of a molecule. This technique measures the electromagnetic radiation emitted from nuclei of a specific atom (usually ^{1}H or ^{13}C) after being exposed to a magnetic field, and notes the chemical shift (δ) of each signal emitted. Identical atoms will all record the same shift, however depending on what the atom is bonded to the effects of that bond, including shielding effect of the bonded atom, will be shown by a signal at a different chemical shift. An understanding of an atoms environment can be gained by looking at the entire spectrum of chemical shifts for that specific atom in a given molecule. This allows for the development in understanding the structure of that molecule.

1.5.2. Rheology

Rheology is the study of the flow of a material.[79,80] It is a complex theory which takes into account a variety of principles and techniques to measure a materials deformity due to an applied force. This study will concentrate on shear force, which is a deformation due to a sliding pressure on a materials layers. These results allow for the calculation of the viscous and elastic components of a material.

Many different rheometer designs exist which can apply a variety of forces; the rheometer in this study is a cone/plate design. The substance being tested is placed between two plates in the rheometer, one as a fixed base plate and the other an oscillating top plate. As the top plate in the rheometer oscillates, the elastic component will be in phase with the movement (phase shift $\delta = 0^{o}$). This is measured as the storage modulus (G') and is generally caused by the polymer network in

hydrogels. The viscous component will be out of phase with the oscillation (phase shift angle δ = 90°). This is measured as the loss modulus (G") and is caused by the water portion of a hydrogel. Most materials are viscoelastic in nature, meaning their phase shift δ is somewhere between 0° and 90° (Fig 1.9).

The above information can be used to understand the gelation process of a material. As the phase angel varies depending on the viscosity or elasticity of a material, the tangent of this angle can provide information about the degree of gelation.

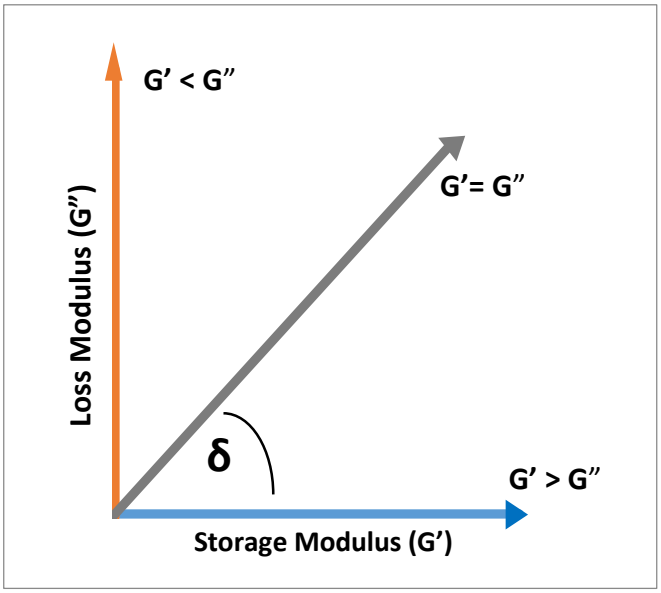

Figure 1.9: An example of G' vs G" showing the tangent angle

Therefore, a 45° angle will mean G'= G" which is the sol-gel transition point. Using this information, the gelation of a gel can be tracked using the equation,

$$tan\ \delta = \frac{G\prime}{G"}, \qquad (2)$$

where large *tan δ* indicated the material is a firm, elastic gel and a small *tan δ* indicates the material is a fluid like gel or liquid. The gelation point of a material is measured when tan δ = 1.

The storage modulus can also provide information about the time required to cure a hydrogel. The storage modulus will continuously increase in magnitude until the material is fully cured. Comparing the storage modulus of different materials can also give us an indication of the potential robustness of a material.

1.5.3. Mechanical Testing

Tensile testing is a technique that involves deforming the material by applying a tensile force to a thin strip of material held between two grips (Fig. 1.10). The test measures the force on the material required to maintain deformation as the stroke is increased at a contact rate.

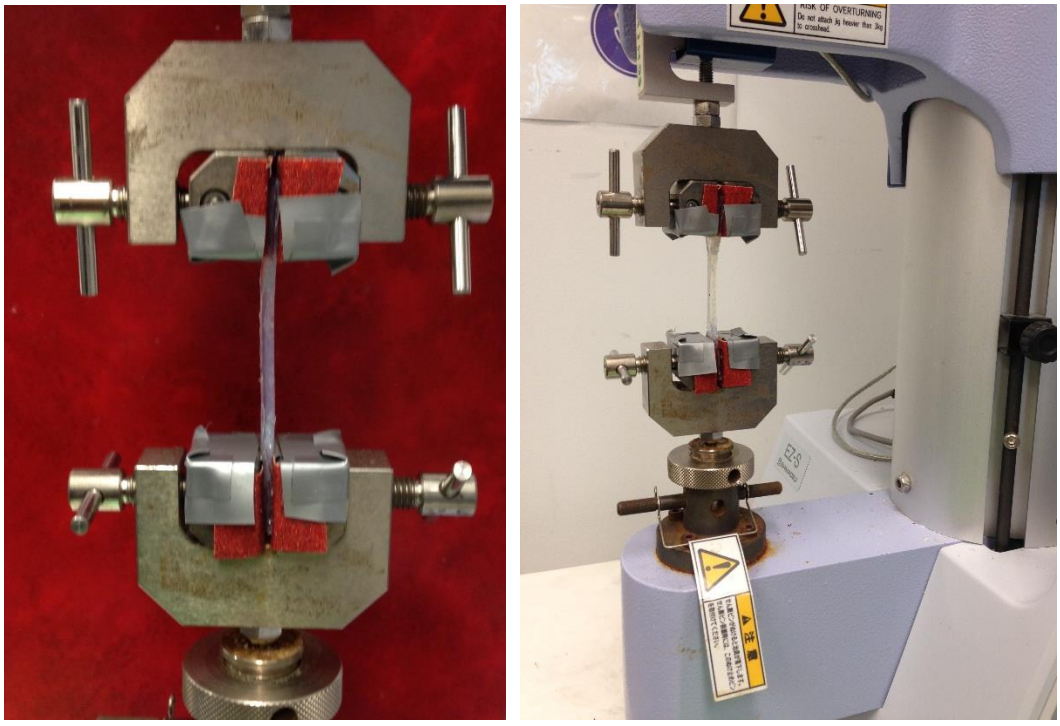

Figure 1.10: Images of universal mechanical analyser tensile testing a hydrogel sample

This data allows for the creation of a stress-strain curve (Fig 1.11) and for the calculation of the mechanical properties using the following equations. Tensile stress (σ_t) is obtained by,

$$\sigma_t = \frac{F}{A}, \tag{3}$$

Where F is the applied force and A is the cross-sectional area. Tensile strain (ε_t) is obtained by,

$$\varepsilon_t = \frac{\Delta l}{l_0}, \tag{4}$$

where Δl is the stroke and l_0 is the original height of the gel. Then the tensile work to failure (W_t) is obtained by,

$$W_t = \int \sigma \, d\varepsilon, \tag{5}$$

and the tensile modulus (E_t) is obtained by,

$$E_t = \frac{\Delta \sigma}{\Delta \varepsilon}. \tag{6}$$

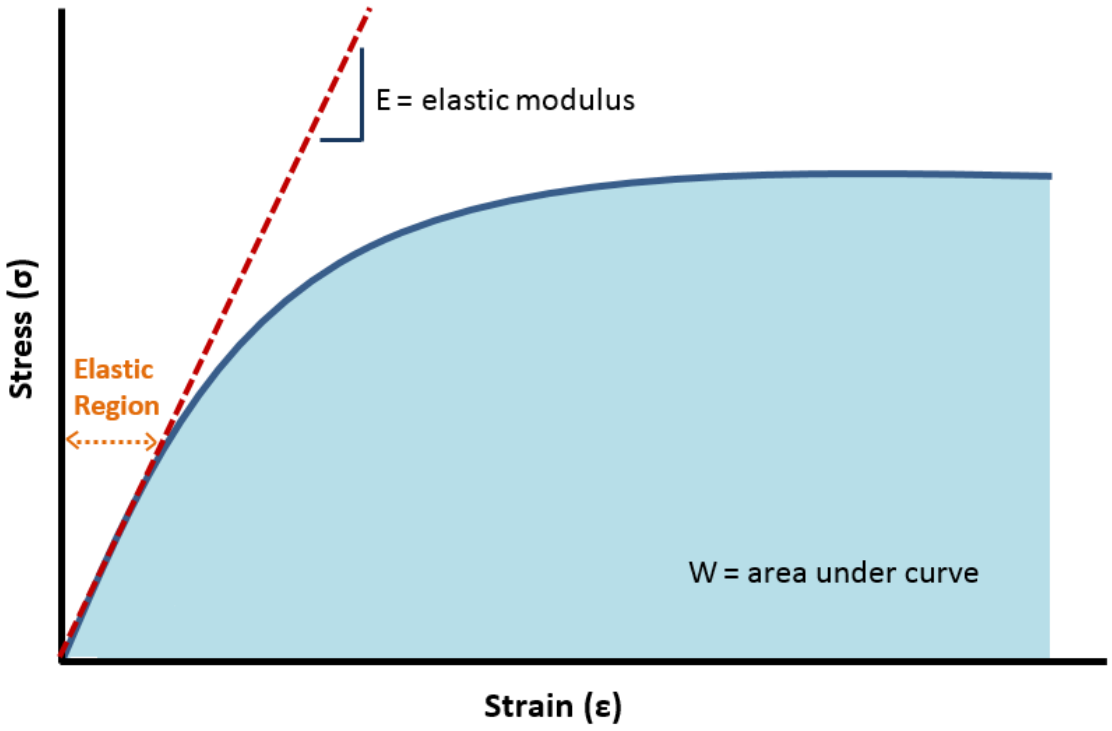

Figure 1.11: An example of a typical stress strain curve for a viscoelastic material

Taking the point of failure of the force, stroke, the cross sectional area, and original length the following values can be calculated; tensile stress at failure (σ_t), tensile strain at failure (ε_t), and work of fracture at failure (W_t). The elastic modulus (E_t) is calculated by taking the slope of the first linear region on the stress-strain plot after the origin.

Compression testing is a technique that involves compressing a material between two fixed plates. This test measures the force applied to the material and stroke at a constant rate of deformation. This data is then treated similarly to that described previously for tensile testing, using equations 3-6 to obtain the compressive stress at failure (σ_c), compressive strain at failure (ε_c), work of fracture (W_c), and elastic modulus (E_c).

1.5.4. Swelling Tests

One of the main benefits of hydrogels are their ability to absorb water. As discussed above this is affected by different structural factors and hence investigating this ability can provide an insight to the hydrogels structure. There are two important calculations for this investigation as discussed below.

The swelling ratio (SR) of the hydrogel can be calculated by the following equation,

$$SR = \frac{W_t}{W_d}, \tag{7}$$

where W_t is the total weight of the swollen hydrogel and W_d is weight of the dried hydrogel. This equation expresses the ability of a hydrogel to swell.

The degree of swelling can be calculated by the equilibrium water content (EWC) by the equation below,

$$EWC = \frac{W_w}{W_t} \times 100\%, \tag{8}$$

where W_t is the total weight of the swollen hydrogel and W_w is the weight of water in the hydrogel. This equation tells us the weight by weight water content of the swollen hydrogel.[37]

1.6. Rapid Prototyping

Rapid Prototyping is a manufacturing technique used to fabricate 3D objects. The object shape is created using computer aided design (CAD) programming and is printed using a layered approach known as 'additive layer manufacturing' (Fig 1.12).[23] The benefit of this approach is that it reduces production time and allows for the manufacturing of complex design or small batches of specific products in a cost efficient manner.[22]

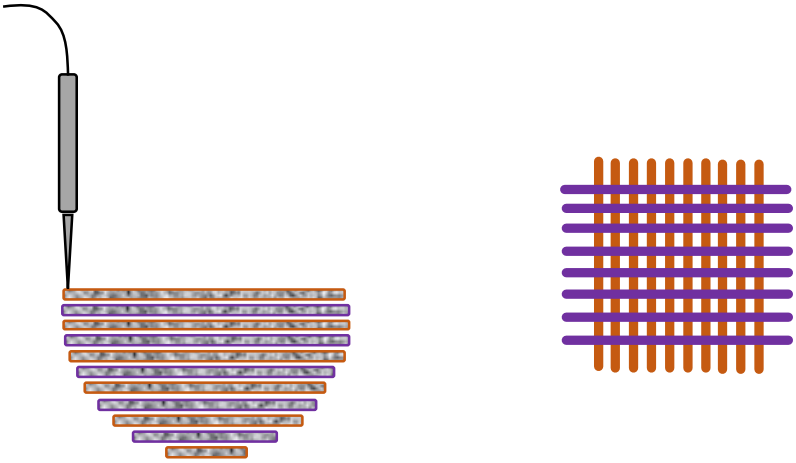

(a) (b)

Figure 1.12: An example of the additive layer manufacturing method for production of 3D objects where (a) shows a layered approach to printing a 3D structure and (b) is an example of the lattice arrangement of the different layers that give support to the overall structure

Additive layer manufacturing requires each layer of the printed material to have structural stability prior to the next layer being printed.[81] In current printing methods, this stability typically comes from the crosslinking process, hence individual layers of the material are crosslinked prior to further

development of the 3D structure.[26–28,82] This method can create weaknesses between individual layers that are not present in similar casted gels and also increases the time required to print the full structure due to the requirement of regular printing stoppages to cure each layer.

The requirement to have a structurally stable base layer throughout this process can also create difficulty for hydrogels produced through two-pot synthesis. This difficulty arises when the first network is required to crosslink prior to the second network being added[56] and would considerably slow down the additive layer manufacturing process.

Extrusion printing is a specific type of rapid prototyping where viscous ink is extruded from a syringe to form parallel lines into a pre-designed shape. There are three types of design for this printing system. In this study, the syringe is kept in a fixed position while the base that the material is printed on is directed in all three axis by a pre-programmed computer system. A non-Newtonian shear thinning fluid is placed in the syringed. The ink is displaced when the force of the syringe plunger is exacted on the material. The plunger mechanism is also controlled by a pre-programmed computer system. Multiple layers are printed on the same x-y base by lowering the base in the z direction after each layer.[23] Similar systems keep the base fixed and move the syringe in all three axis or move the base in the x-y axis and the syringe in the z axis to create the same result.[83]

Additional mechanical components may be added to the system depending on the ink characteristics. Examples include heated or cooled base plates for thermoresponsive inks, UV light sources for photocurable inks, and time delay systems.[81]

As these systems are dependent on the ink having pseudo-plastic (non-Newtonian) properties, rheological analysis of the flow curve of the material with a varying shear rate are required prior to printing. These measurements can be fitted to the power law model to investigate the shear

thinning properties of the material. The viscosity of the material is measure over a variable shear rate and fitted to the power law equation,

$$\eta = K\dot{\gamma}^{n-1}, \quad (9)$$

where η is the viscosity, K is the consistency index, $\dot{\gamma}$ is the shear rate, and n is the power law index. The behaviour of a fluid is described by the power law index; where n > 1 is a dilatant, n = 1 is a Newtonian fluid, and n < 1 is a non-Newtonian pseudo plastic.[80]

1.7. Aims

There is a constant need for research and development of new materials for modern application that can be manufactured through rapid prototyping. The main aim of this thesis is to synthesis and characterise a new mechanically robust double network 3D printable gelatin – epoxy amine hydrogel. This will be accomplished by the following objectives.

1. To develop a double network photo curable gelatin - epoxy amine based hydrogel with a mechanical strength greater than either of the individual networks.

2. To gain an understanding of the chemistry of the gelatin - epoxy amine based hydrogel final product and the variation of chemistry of the different syntheses methods used to produce the hydrogel.

3. To optimise the gelatin - epoxy amine hydrogels through their structural variables; polymer content, polymer ratio, choice of methacrylate, synthesis method (one-step and two-step), and choice of curing agent.

4. To optimise the hydrogels rheological properties required for 3D printing to allow the hydrogel act as a printable ink for rapid prototyping.

2. Materials and Methods

2.1. Materials

The hydrogels in this study were produced using the monomers gelatin, (from porcine skin, Sigma Aldrich, USA, ~300g bloom, type A, molecular weight 87.5kDa, lot number SLBK6158V) and Jeffamine® ED 2003, (Huntsman, USA, amine meq/g 0.9 min. – 1.05 max., approximate molecular weight 2000 g/mol, lot number 2M707).

The two methacrylates used in this study were glycidyl methacrylate, (97%, contains 100 ppm monomethyl ether hydroquinone as inhibitor, Sigma Aldrich, USA, molecular weight 145.15 g/mol, lot number BCBK5528V) and methacrylic anhydride, (contains 2,000 ppm topanol A as inhibitor, 94%, Sigma Aldrich, USA, molecular weight 154.16 g/mol, lot number STBD2085V).

The four curing agents used in this study were Irgacure 2959 (Ciba Specialty Chemicals Inc., 1-[4-(2-Hydroxyethoxy)phenyl]-2-hydroxy-2-methyl-1-propane-1-one, molecular weight 224.3 g/mol), Irgacure 819 (Ciba Specialty Chemicals Inc., Bis(2,4,6-trimethylbenzoyl)-phenylphosphineoxide, molecular weight 418.5 g/mol), Thioxanthen-9-one (97%, Sigma Aldrich, USA, molecular weight 212.27 g/mol, Lot Number BCBB3891V), and Diphenyl (2,4,6-trimethylbenzoyl)phosphine oxide) (97%, Sigma Aldrich, USA, molecular weight 348.37 g/mol, lot number MKBP8673V).

All hydrogels were made with Milli-Q water (resistivity, 18.2 MΩ cm, Millipore, USA). Where ethanol is required this was purchased from Ajax Finechem, Australia.

2.2. Solution Preparation

To produce the Irgacure 2959 solution, 10ml of ethanol was added to 0.01g of Irgacure 2959 in a 10ml Eppendorf tube. The mixture was vortexed for approximately 30 seconds until the powder dissolved.

To produce the Irgacure 819 solution, 10ml of ethanol was added to 0.01g of Irgacure in 10ml an Eppendorf tube. The mixture was vortexed for approximately 30 seconds until the powder dissolved.

To produce the Tx91 solution, 10ml of ethanol was added to 0.00016g of Thioxanthen-9-one in a 10ml Eppendorf tube. The mixture was vortexed for approximately 30 seconds until the powder dissolved.

To produce the Dp246 solution, 10ml of ethanol were added to 0.0023g of Diphenyl (2,4,6-trimethylbenzoyl)phosphine oxide) in a 10ml Eppendorf tube. The mixture was vortexed for approximately 30 seconds until the powder dissolved.

2.3. Synthesis

2.3.1. Gelatin-Methacrylate

Gelatin-methacrylate with a total polymer content of 20% was produced as follows. 40ml of Milli-Q was measured using a graduated cylinder, placed in a 100ml beaker, and heated on a magnetic hot plate (Stuart CB162) at 40 °C. The water was maintained at this temperature and vigorously stirred using a magnetic stirring bead while 8.33g of gelatin was added over a period of up to 20 seconds. The mixture then gently stirred for approximately 20 minutes until the gelatin had completely

dissolved. Stirring was then stopped and 2-3 drops of ethanol were added to the beaker to break the surface tension and ensure any air bubbles were destroyed. The gentle stirring then resumed while 1.67ml of glycidyl methacrylate (or methacrylic anhydride) was added to the beaker. After two minutes, the solution was poured into a 50ml centrifuge tube, sealed and placed in an oven (Thermoline Scientific) at 40 °C (or 60 °C for methacrylic anhydride) for up to 18 hours.

The ratio of gelatin to methacrylate was consistently kept at 1:0.2 throughout the research project. The amount of gelatin and methacrylate varied depending on the polymer percentage required in the final product. For variations on the total polymer content see Appendix 1.

2.3.2. ED2003-Methacrylate

ED2003-GMa with a total polymer content of 20% was produced as follows. 40ml of Milli-Q was measured using a graduated cylinder, placed in a 100ml beaker, and heated on a magnetic hot plate at 40 °C. The water was maintained at this temperature and gently stirred while 8.24ml of ED2003 was added over a period of up to 10 seconds. The mixture was continually stirred for approximately 5 minutes until the ED2003 had dispersed. 1.17ml of glycidyl methacrylate was added to the beaker. After two minutes, the solution was poured into a 50ml centrifuge tube, sealed and placed in an oven at 40 °C for up to 18 hours.

ED2003-MAh with a polymer content of 20% was produced in similar fashion by using 8.73ml of ED2003 and 0.67ml of methacrylic anhydride. When using MAh, the oven is set to 60 °C. For variations in polymer content for both materials, see Appendix 1.

2.3.3. One-step synthesis of gelatin-ED2003-methacrylate hydrogels

One-step gelatin-ED2003-Gma with a total polymer content of 20% was produced as follows. 40ml of Milli-Q was measured using a graduated cylinder, placed in a 100ml beaker, and heated on a magnetic hot plate at 40 °C. The water was maintained at this temperature and vigorously stirred using a magnetic stirring bead while 6.67g of gelatin was added over a period of up to 20 seconds. The mixture then gently stirred for approximately 20 minutes until the gelatin had dissolved at which point the stirring was stopped and 2-3 drops of ethanol were added to the beaker to break the surface tension and ensure any air bubbles were destroyed. While continuing a gentle stir, 1.65ml of ED2003 was added over a period of up to 10 seconds. The mixture was continually stirred for approximately 5 minutes before 1.51ml of glycidyl methacrylate was added to the solution. After 2 minutes the solution was poured into a 50ml centrifuge tube, sealed and placed in an over at 40 °C for up to 18 hours.

The volumes of gelatin, ED2003, and methacrylate varied depending on the required product. When using MAh the oven is set to 60 °C. See Appendix 1 for a full range of variants.

2.3.4. Two-step synthesis of gelatin-ED2003-methacrylate hydrogels

Gelatin-GMa with a polymer content of 20% was produced as follows. 20ml of Milli-Q was measured using a graduated cylinder, placed in a 50ml beaker, and heated on a magnetic hot plate at 40 °C. The water was maintained at this temperature and vigorously stirred using a magnetic stirring bead while 8.33g of gelatin was added over a period of up to 20 seconds. The mixture then gently stirred for approximately 20 minutes until the gelatin had dissolved at which point the stirring was stopped and 2-3 drops of ethanol were added to the beaker to break the surface tension and ensure any air bubbles were destroyed. The gentle stirring then resumed while 1.67ml of glycidyl methacrylate was

added to the beaker. After two minutes, the solution was poured into a 50ml centrifuge tube, sealed and placed in an oven at 40 °C for up to 18 hours.

Concurrently, ED2003-GMa with a polymer content of 20% was produced as follows. 20ml of Milli-Q was measured using a graduated cylinder, placed in a 50ml beaker, and heated on a magnetic hot plate at 40 °C. The water was maintained at this temperature and gently stirred while 8.24ml of ED2003 was added over a period of up to 10 seconds. The mixture was continually stirred for approximately 5 minutes until the ED2003 had dissipated. 1.17ml of glycidyl methacrylate was added to the beaker. After two minutes, the solution was poured into a 50ml centrifuge tube, sealed and placed in an oven at 40 °C for up to 18 hours.

After 15-18 hours had passed, the contents of the centrifuge tube containing the ED2003-GMa were added to the tube containing the gelatin-GMa. This tube was then sealed and hand rotated 5 times to allow the two solutions to mix.

The volumes of gelatin, ED2003, and methacrylate varied depending on the required product. When using MAh the oven is set to 60 °C. See Appendix 1 for a full range of variants.

2.4. Photo curing and characterisation

Prior to any characterisation tests taking place, a photoinitiator was added to the products produced as discussed. The volume of photoinitiator added varied depending on the agent used and are listed in Appendix 1. When the photoinitiator had been added, the centrifuge tube was inverted by hand to disperse the agent throughout the solution.

This solution was then cured using a UV light source (Dymax BlueWave 75 Rev 2.0 UV Light Spot Lamp) at approximately 19+ W/cm^2 at 280nm with the source placed 3cm above the hydrogel.

For rheology testing, the UV box was connected directly to the rheometer as discussed below and each sample was cured for 60 seconds or as testing required. To prepare the hydrogels for compression testing, each 10mm high, 15mm diameter cylinder was cured for 5 minutes using the UV source. To prepare the hydrogels for tensile testing, the gel solution was poured into an 81mm x 81mm base weigh boat and each 27mm x 27mm sector was cured for 5 minutes using the UV source.

2.4.1. Rheology

Rheology analysis was performed using a rheometer (Anton Paar Physica MCR301Digital) with a cone and plate measuring system (49.972 mm diameter, 0.992 angle, 97 mm truncation), a temperature controlled stage (AWC100, Julabo, Germany) maintained at 40 °C (or as indicated) supported by a temperature controlling hood, and a UV source as discussed above. The data obtained was processed as previously discussed.

2.4.2. Mechanical Testing

Compression and tensile analysis were performed using a universal mechanical tester (Shimazdu EZ-S with coupled software, Trapesium) at approximately 21°C.

Compression test samples were prepared using a 10mm high circular mould with a 15mm diameter at a compression rate of 1mm/min. The measurements obtained were processed as previously discussed.

Tensile test samples were cut using a dumbbell cutter (total length: 7.5cm, middle strip length: 3cm, middle strip width: 4mm) and were extended at a rate of 10mm/min. The measurements obtained were processed as previously discussed.

2.4.3. Swelling Tests

All hydrogels prepared in this test had a total polymer content of 20% and a polymer ratio of G(80%):E(20%). Gelatin-ED2003-MAh and gelatin-ED2003-GMa solutions using both one-step and two-step methods were prepared as previously discussed. The hydrogels were set and cured as previously discussed in preparation for compression testing.

The hydrogels were weighed on a weighting balance (PB3002-s/FACT, Mettler Toledo, Australia) and placed in 75ml Milli-Q water in a 100ml beaker for four days at approximately 21°C. They were then removed and both sides were gently placed on a piece of Kim Teck wipe to remove any excess water. The gel was then weighed and placed in a petri dish in a 40 °C oven for four days.

2.4.4. Spectroscopic analysis

All hydrogels solutions were prepared and cured as previously discussed in preparation for compression testing.

FTIR analysis was performed using a Fourier transform infrared spectrometry (IRAffinity-1, Shimadzu, Australia). Samples were prepared as above and placed directly in the FTIR machine for analyses.

^{1}H and ^{13}C NMR spectra were recorded in D_2O (D, 99.96%, Cambridge Isotope Laboratories, Inc) at 30°C, on a Bruker Advance III 400 MHz system. ^{1}H and ^{13}C signals are recorded in parts per million (ppm). Samples were prepared as above in any placed in a 120 °C oven for 48 hours to remove all water. The hydrogels polymer content were then ground down and placed in an NMR tube to fill 5mm of the tube. Deuterium oxide was added until the mixture filled 2cm of the tubing and the sample was then analysed.

2.4.5. 3D Printing

Extrusion printing was carried out using a custom-built 3D Printer. The instrument consisted of a Sherline 8020 CNC milling stage controlled by a LinuxCNC computer system and a 5ml syringe with a 25GA tip (EFD, Lot/SN: 4000276262) controlled by a Zaber pump step motor using a Zaber console on a second computer system.

The gel solution was added to the syringe and allowed to cool for 5 minutes prior to printing. Photopolymerisation was carried out post printing using a UV light source (Dymax BlueWave 75 Rev 2.0 UV Light Spot Lamp) at approximately 19+ W/cm^2 at 280nm with the source places 3cm above the hydrogel.

2.5. Statistical Treatment

Rheology data reported are average values from triplicate experiments. Mechanical data has been calculated as the average of between five and ten consecutive tests. All errors in this report have been found by calculating one standard deviation of the mean. Data results have been rounded to the nearest whole number.

3. Results and Discussion

Hydrogel networks with contrasting properties have been combined to form robust hydrogel networks called Double Network hydrogels. This study will look at a new combination of networks. Gelatin can be considered a weak, elastic network, whereas Jeffamine® ED2003 is a tough, brittle network. This study examines the initial development and characterisation of these gels with some investigation into the internal chemistry of the crosslinked networks and synthesis reactions.

This section will discuss the comparison of two one-pot synthesis methods, a one-step process and a two-step process, and two different methacrylates, Glycidyl Methacrylate (GMa) and Methacrylate Anhydride (MAh), with respects to the production of gelatin-ED2003-methacrylate hydrogels. To compare these samples, the hydrogel properties were tested using rheology, mechanical testing, and swell testing. The structure of the hydrogels was investigated using NMR and FTIR techniques. The hydrogels were printed using extrusion techniques to consider the possible applications for this system. The discussion below highlights the main findings.

3.1. Synthesis

Choice of photoinitiator

Rheological and compression testing were conducted to find the optimum photoinitiator to use for the curing process. Four curing agents were tested; Dp246, Tx91, Irgacure 2959, and Irgacure 819.

It was found that Dp246 produced hydrogels with the highest maximum storage modulus at 28 ±0.1 kPa (Table 3.1). From physical observation both the Irgacure 819 and Dp246 hydrogels appeared to produce more evenly cured hydrogels. This meant that the curing throughout the hydrogel was consistent unlike the Irgacure 2959 and Tx91 hydrogels, which appeared to consist of a wet

transparent bottom level and a dry cloudy top layer. This may be due to the elevated light absorption levels at 280nm of Irgacure 819 and Dp246 are which are higher than Irgacure 2959 and TX91 at the same wavelength allowing the lamps emission spectra to synergise with the absorption rate of the photoiniators.[84]

Table 3.1: Maximum storage modulus (G'_{max}) at 30 minutes, compressive stress at failure (σ_c), compressive strain at failure (ε_c), work of fracture (W_c), and elastic modulus (E_c) of G(60%):E(40%) MAh hydrogels prepared by one-step synthesis with a TPC of 20%.

Photoinitiator	**G'_{max}**	**σ_c**	**ε_c**	**W_c**	**E_c**
	(kPa)	(kPa)	(%)	(kJ/m^3)	(kPa)
Irgacure 2959	6 ±0.08	161 ±9	60 ±1	29 ±1	206 ±12
Irgacure 819	5 ±0.1	236 ±10	81 ±3	52 ±7	77 ±5
Dp246	28 ±0.1	1913 ±548	95 ±20	160 ±38	56 ±8
Tx91	4 ±0.03	296 ±41	92 ±9	35 ±8	0.1 ±0.01

Initial compression testing was also performed on the same hydrogel using the four different photoinitiators. The results in Table 3.1 show that DP246 produces hydrogels with the highest compressive stress to failure, compression strain to failure, and work of fracture. This supports the rheological data listed in the same table. Dp246 will continue to be used as the photoinitiator for the remainder of this study.

Establishing the percentage of Total Polymer Content

Rheological testing was carried out on gelatin-MAh with a varying percentage of polymer content to establish the optimum Total Polymer Content (TPC) for production of these hydrogel systems. Fig 3.1 shows that storage modulus (G'_{max}) increased with increasing polymer content, hence the robustness of a hydrogel can be manipulated by the volume of polymer content. As the TPC increases the solutions become more viscous and difficult to produce. The highest TPC that was producible for both gelatin-MAh and gelatin-GMa was at 25% whereas this went up to 40% for ED2003-MAh and

ED2003-GMa. However, as mentioned above, the solutions produced at these respective TPC's were highly viscous and hence difficult to reproduce. Due to this difficulty, hydrogels tested hereafter had a TPC of 20% with a varying ratio of gelatin-GMa to ED2003-GMa and gelatin-MAh to ED2003-MAh.

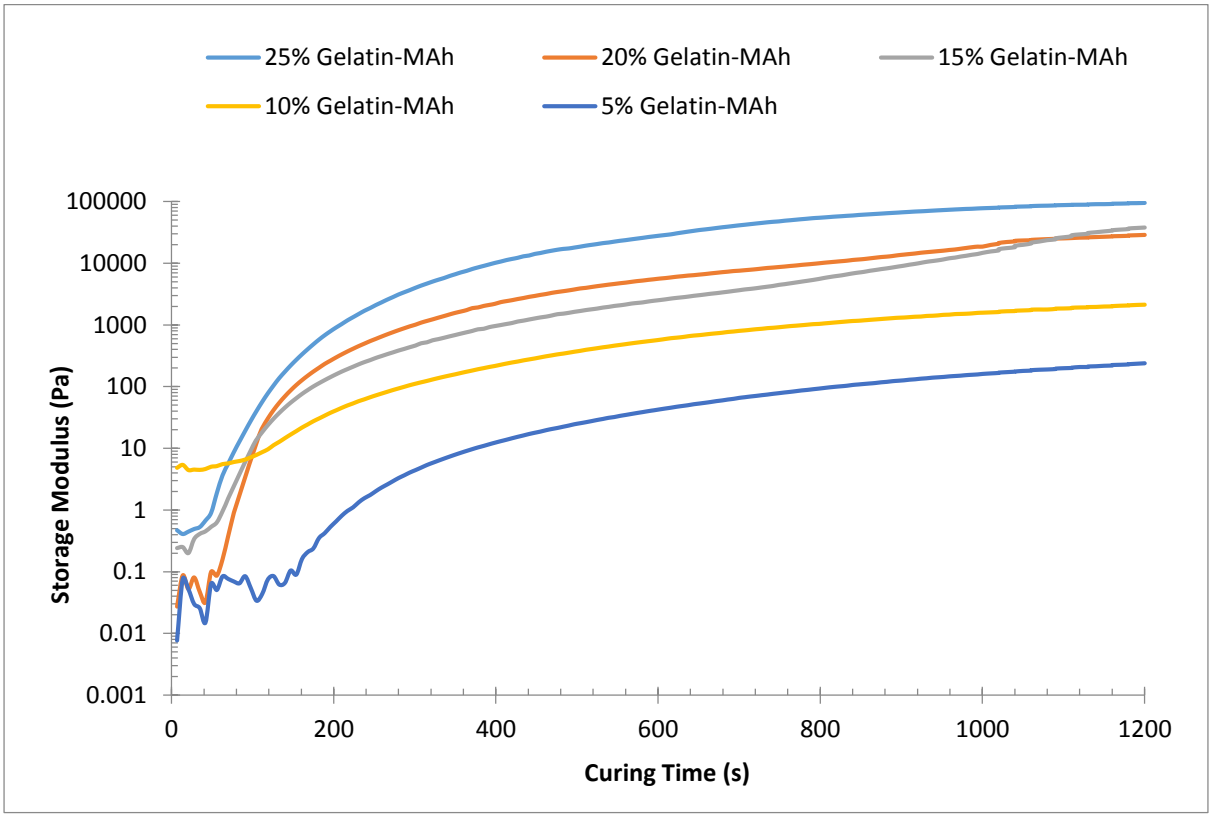

Figure 3.1: Typical change in storage modulus as a function of curing time for gelatin-MAh hydrogels prepared using one-step synthesis with varying total polymer content. Data collected at 40°, frequency = 1Hz, and strain = 1%. Samples were continuously exposed to UV light from 30 seconds after the experiment began.

Choice of methacrylate

Methacrylates can be used as crosslinkers between polymer chains. They will react and link onto a polymer over a specified period of time. Further to this, with the additional of a curing agent and in the presence of UV light, they will react with each other to create the crosslink between the chains they are linked to. This study will compare two different methacrylates; Methacrylic Anhydride (MAh) and Glycidyl Methacrylate (GMa).

Synthesis method

Double Network hydrogels can be produced using a variety of methods. This study will use a one-pot synthesis method and compare a one-step method and a two-step method. The one-step method occurs when the two polymer networks are methacrylated in the same reactor and then cured. The two-step method occurs when the two polymer networks are methacrylated separately and then combined before being cured. Two-step synthesis is likely to produce a purer double network hydrogel as the networks are not able to react with each other during methacrylation. The one-step method is more likely to produce mixed networks due to the variety of functional groups on both the gelatin and ED2003 that can react with other during the methacrylation process. A more detailed understanding of these reactions can be gained from fourier transform infrared (FTIR) spectroscopy and nuclear magnetic resonance (NMR) spectroscopy.

3.2. Spectroscopy

From initial observation it can be seen that one-step method produces more transparent gels than two-step method (Fig 3.2). This indicates that there is potentially a double phase in the two-step hydrogels which is not present in the one-step hydrogels. The double phase may be due to colloidal properties still being present in the two-step hydrogel after they are cured. It may also be due to the ED2003-MA and gelatin-MA curing as separate networks at different times creating different gel phases.

Images of the dehydrated hydrogels are shown in Fig 3.3. It was noted that all four hydrogels appear physically different when dehydrated. The GMa hydrogels hold their structure better while the MAh hydrogel collapsed in at the sides suggesting that the internal structure at these points is not

crosslinked in the same manner as is at the top of the hydrogel. The colour of the one-step is also much richer than that of the two-step hydrogels.

Both of these images indicated the internal structure of theses gels varies depending on the choice of methacrylate and the synthesis method used. FTIR and NMR analysis was used to analyse the internal structure of these hydrogels to gain a more thorough understanding of their internal structure.

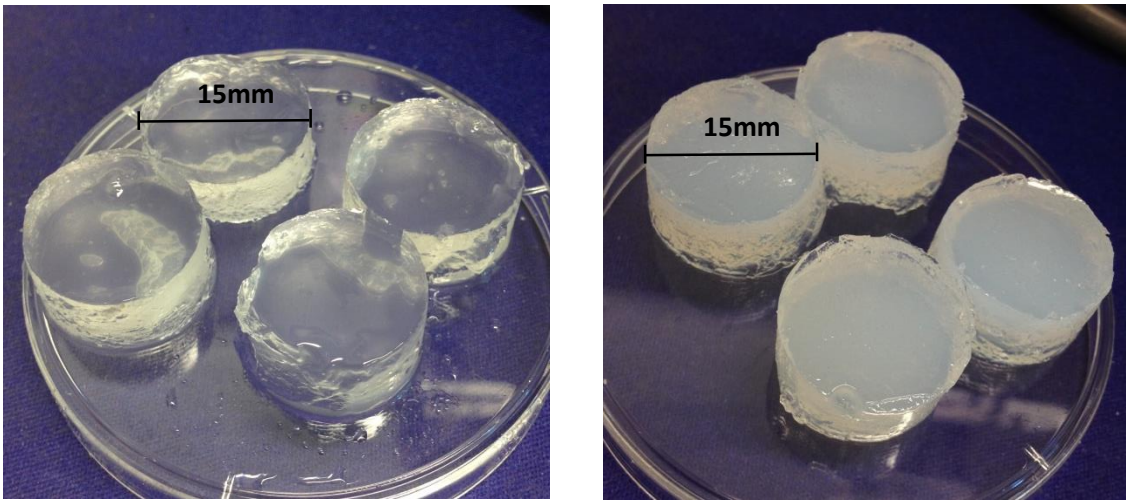

(a) *(b)*

Figure 3.2: G(80%):E(20%) GMa hydrogels with a TPC of 20% produced by (a) a one-step method and (b) a two-step method.

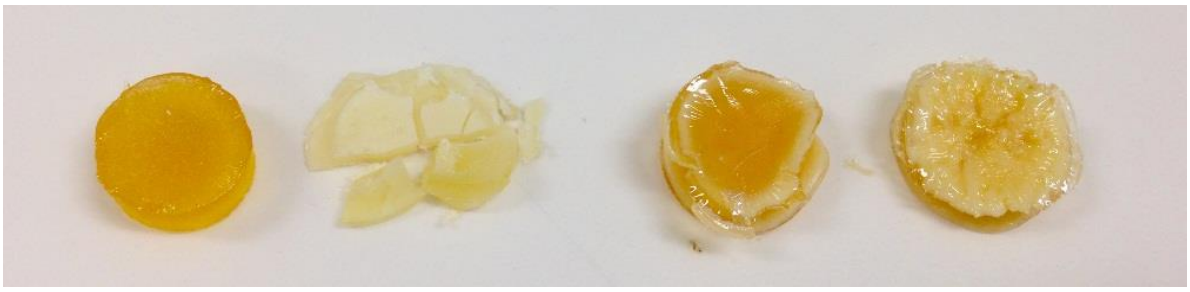

Figure 3.3: Images of typically dehydrated G(80%):E(20%) hydrogels with a TPC of 20%. (left-right: GMa & one-step synthesis, GMa & two-step synthesis, MAh & one-step synthesis, MAh & two-step synthesis)

FTIR analyses

This experiment investigates the FTIR of gelatin, ED2003, gelatin-MAh, ED2003-MAh, and gelatin-ED2003-Mah (G(80%):E(20%)) by one-step synthesis. As these are hydrogel products water is the main solvent in all of the above mentioned solutions. This impedes the response in the 3000-4000 nm region of the spectra.

ED2003 vs ED2003-MAh

The ED2003-MAh spectrum showed a decreased peak at 2881 nm and 1080 nm and an increase at 1639 nm compared with ED2003 (Fig A6.2). A decrease at 2881 nm is associated with a reduction of carbon hydrogen single bonds. A reduction at 1080 nm may be due to a reduction in the C-O bonds or a reduction in C-N linear bonds. Both of these suggest that the MAh may not only be reacting with the amine but with other areas of the ED2003. A wider variety of testing is needed to clarify these changes. The additional peak at 1639 nm is most likely the introduction of the C=C bond from the methacrylic anhydride or methacrylic acid as the anhydride reacts with the water.

If the methacrylic anhydride is reacting with the ED2003 at the amine functional group, it would be expected that an amine to amide change would be visible. However, it is not possible to clarify if this change occurs as the amide region is consumed by the water in the mixture. This change may be easier to see with NMR spectroscopy.

Gelatin vs Gelatin-MAh

The gelatin-MAh spectrum shows a change in peak size at 945 nm, 1002 nm, 1454 nm, and 3394 nm compared with the gelatin spectrum (Fig A6.1). However, this last peak is consumed by the water signal and cannot be taken as an accurate reading. The 945 nm peak indicated the introduction of the methacrylic anhydride as it is breaking up to form to carboxyl groups. Similarly, the 1002 nm and 1454 nm peaks most likely represents the addition of the hydrogens attached to carbon double

bonds on the methacrylic anhydride and changes to the current carbon hydrogen bonds within the gelatin molecule. There is a general increase in bonds in the 1000-2000 nm region. This is most likely due to the variety of bonds created with the gelatin molecule, however their peaks are not clear enough to pick out specific changes.

Gelatin-ED2003-MAh by one-step synthesis

The gelatin-ED2003-MAh spectrum did not show the introduction of any new bonds in the 1000-3000 nm region (Fig A6.3). Beyond this, water signals block the results. Slight variations of peak sizing occurs but no new bonds seem to be created. However, this spectrum has more similarities to the gelatin-MAh spectrum than to the ED2003-MAh spectrum. This is due to the larger percentage of gelatin-MAh present in the product.

NMR analyses

Due to the lack of clarity from the FTIR primarily due to water interference, ^{13}C NMR was used to investigate gelatin, ED2003, gelatin-ED2003-GMa, and gelatin-ED2003-MAh in the presence of D_2O (Fig. A5.1 and Fig. A5.2).

G(80%):E(20%) GMa – one-step and two-step syntheses

The spectra for both syntheses methods using GMa are quite similar. Both hydrogel products are absent of the ED2003 amine peak (~ 45-46 ppm), which indicates that the ED2003 has fully reacted. The GMa ring signal is also absent in the final product (~ 125-150 ppm), meaning the GMa rings have opened and reacted as expected. However, a reduction in some of the functional groups off the ED2003 backbone is also noted (~ 60-80 ppm). Further investigation is need to understand this change.

G(80%):E(20%) MAh – one-step and two-step syntheses

The spectra for both syntheses methods using MAh are also quite similar. The complex gelatin and ED2003 backbones are still present and show only slight peek width variations (~ 60-80 ppm). However, a difference in the relative heights of the MAh carbon peaks was noted (~ 120-140 ppm). The C-O bonds (~ 160 ppm) and C=C double bonds (~ 140 ppm) are reduced in the one-step method. However, the C=C double bond is not reduced in the two-step method. This shows that the methacrylate is both splitting apart to form methacrylic acid by reacting with water and also reacting at the carbon double bond, hence taking part in more reactions in the one-step synthesis. This could be due to the wider variety of functional groups available for bonding in this synthesis method. A complete withdrawal of the ED2003 C-N bond was also noted (~ 45-46 ppm), which shows that the ED2003 is reacting fully with all amine functional groups.

G(80%):E(20%) MAh one-step vs G(80%):E(20%) GMa one-step

There is a dramatic different in complexity noted between the products produced using MAh and GMa by one-step synthesis. The MAh hydrogel product gives an erratic signal which indicated a wider variety of reactions are taking place in this hydrogel. The MAh based product by one-step synthesis also has some additional peaks between the 100-180ppm which are indicators of methacrylic acid. This is most likely due to the reaction between MAh and water producing methacrylic acid which is not fully reacting with the polymers or has been trapped within the hydrogel during the curing process.

G(80%):E(20%) MAh two-step vs G(80%):E(20%) GMa two-step

A similar difference in complexity between these two products is also seen in the final spectrums. Again, the MAh is the more complex product which produces an erratic spectrum. Both spectrum contain groupings of broad peaks which indicated there is a wide variety of bonding taking place.

These broad peaks can oppress higher peaks which would otherwise be obvious. Further characterisation tests were carried out to investigate these hydrogel further.

From the above analysis it can be concluded that the hydrogels containing MAh are involved in a wider variety of reactions due to the reaction of the MAh with the water solution, making their structures more complex than the GMa based hydrogels. The one-step synthesis reactions also have more complex structures than the two-step synthesis hydrogels due to a wider variety of reaction site available during the methacrylation process. Further to this, the ED2003 amine is reacting fully as expected and that a variety of the functional group on the gelatin are being reacted. The following sections will discuss the implications that these structural differences have on the characteristics of the different hydrogels.

3.3. Rheology

The epoxy amine-gelatin based hydrogel discussed in this study is first methacrylated in the presence of water to create a colloid which is then photo-cured to create a hydrogel. Unlike the liquid components in this process, the solid components exhibit an elastic property which responds to shear force. This property can be tracked through the rheometer which provides information on the development of the sol-gel transition.

Rheological testing using an oscillating shear force was carried out to determine the storage loss moduli and gelation times of G(80%):E(20%) with either MAh or GMa and produced by one-step or two-step synthesis with a TPC of 20% (Table 3.2). The storage modulus (G') and storage loss (G") were measured with respect to time (example Fig 3.4). This allowed for the calculation of the maximum storage modulus at twenty minutes (G'_{max}), the amount of time required for the sol-gel transition to occur, and the total curing time for each hydrogel (Table 3.2). The point of gelation

occurs when the storage modulus records a greater value that the storage loss. At this point there is more elastic component to the gel than liquid component.

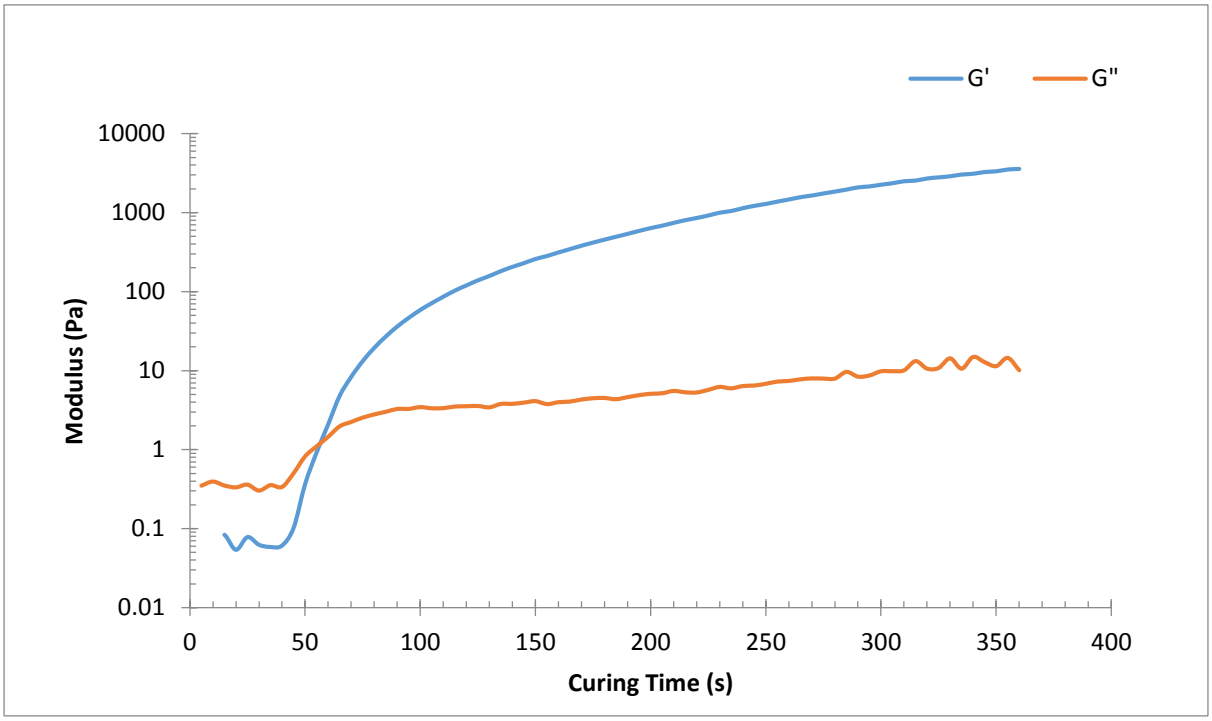

Figure 3.4: Typical storage modulus (G') and loss modulus (G"), as a function of curing time for gelatin-ED2003-MAh hydrogels prepared using one-step synthesis. Data collected at 40°C, frequency = 1Hz, and strain = 1%. Samples were continuously exposed to UV light from 30 seconds after the experiment began.

Table 3.2: A summary of the time at sol-gel transition and maximum storage modulus at 20 minutes for four comparative hydrogels. G(80%):E(20%), TPC 20%, photoinitiator Dp246, produced using either one-step or two-step synthesis with either MAh or GMa as the methacrylate. Samples were continuously exposed to UV light from 30 seconds after the experiment began.

Hydrogel	**Time to gelation** (s)	**G'_{max} at 20 mins** (kPa)
One-step synthesis with MAh	80 ±8	17 ±4
Two-step synthesis with MAh	25 ±20	153 ±43
One-step synthesis with GMa	53 ±6	49 ±2
Two-step synthesis with GMa	70 ±3	60 ±10

These results show that using MAh and a two-step method shortens the time taken to cure the gels. There is no relationship between the synthesis method and the time to gelation. These results must be taken into account when investigating 3D printing application for these hydrogels. The time it takes to cure the hydrogel is important for applying these gels to 3D printing technology, which requires a fast curing gel for its layered approach (see Section 1.6).

Further to this, Fig 3.5 shows the change in storage modulus of the MAh based hydrogels over 20 minutes. Two stages of curing are observed, the first increase in G' occurs in the first 10 mins. A further increase in G' can be seen between approximately 10-20 mins of curing time. This may be due to a variation in curing time between the two polymers with the initial increase relating to the gelatin-MA curing and the second increase relating to the ED2003-MA curing.

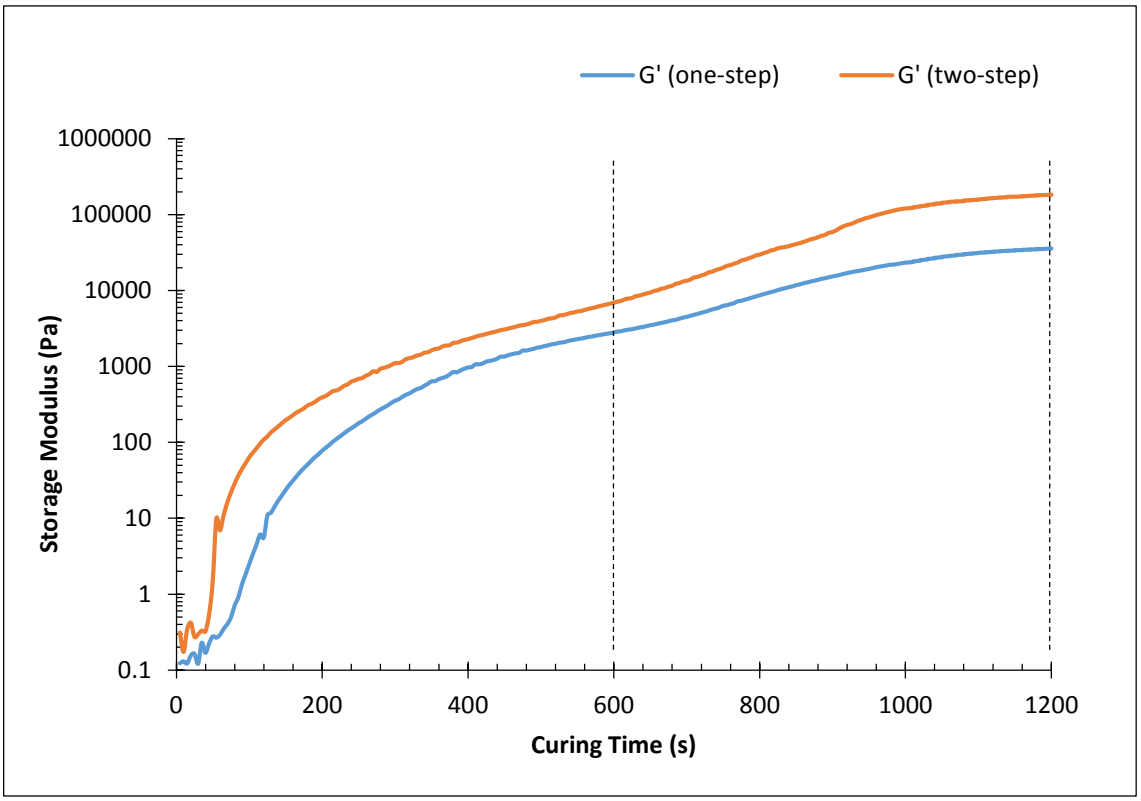

Figure 3.5: Storage modulus (G') over time for G(60%):E(40%) MAh with a TPC of 20%. Data collected at 40°C, frequency = 1Hz, and strain = 1%.

Fig 3.6 (a) shows a comparison between one-step and two-step synthesis of gelatin-ED2003 hydrogels prepared using MAh as a cross-linker. It can be seen that both synthesis methods produced a robust hydrogel in comparison to the individual polymers when the percentage of gelatin-MA in the product is higher than approximately 50%. However, the two-step method produces a significantly higher increase than the one-step method. This may be due to the fact that the ED2003 and gelatin are methacrylated separately so no cross methacrylation can occur, resulting in a purer double network structure. In the one-step method both polymers are methacrylated together which may lead to a single interlinked network system due to the multiple functional groups on each of the two polymer networks.

Similarly, Fig 3.6 (b) shows a comparison between one-step and two-step synthesis of gelatin-ED2003 hydrogels prepared using GMa as a cross-linker. It can be seen that neither synthesis method produces a robust hydrogel in comparison to the individual polymers. From this result we can assume that MAh is a more effective crosslinker than GMa. However, compression testing was carried out on the same gels to confirm this theory.

The highest storage modulus recorded was 168 ±27 kPa for G(60%):E(40%) MAh hydrogels using the two-step method. The above results suggest that combining and methacrylating the gelatin and ED2003 to create a double network hydrogel has the potential to increase the robustness of these hydrogels when using a two-step synthesis method and methacrylating the hydrogels using MAh. To further investigate this potential strength, testing was carried in the form of compression, swelling, and tensile testing.

(a)

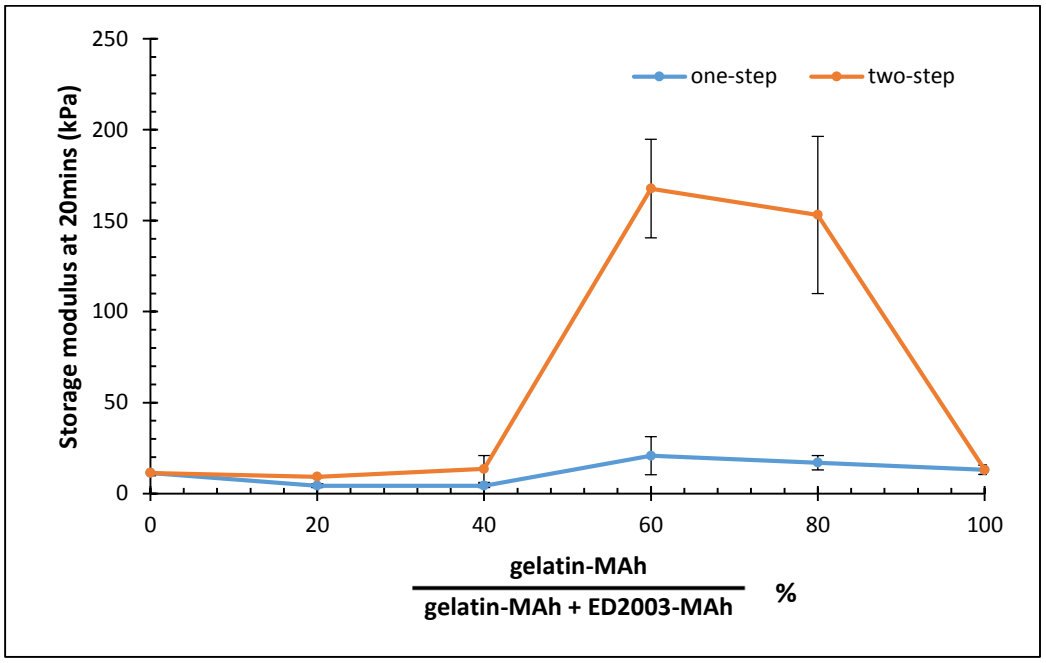

(b)

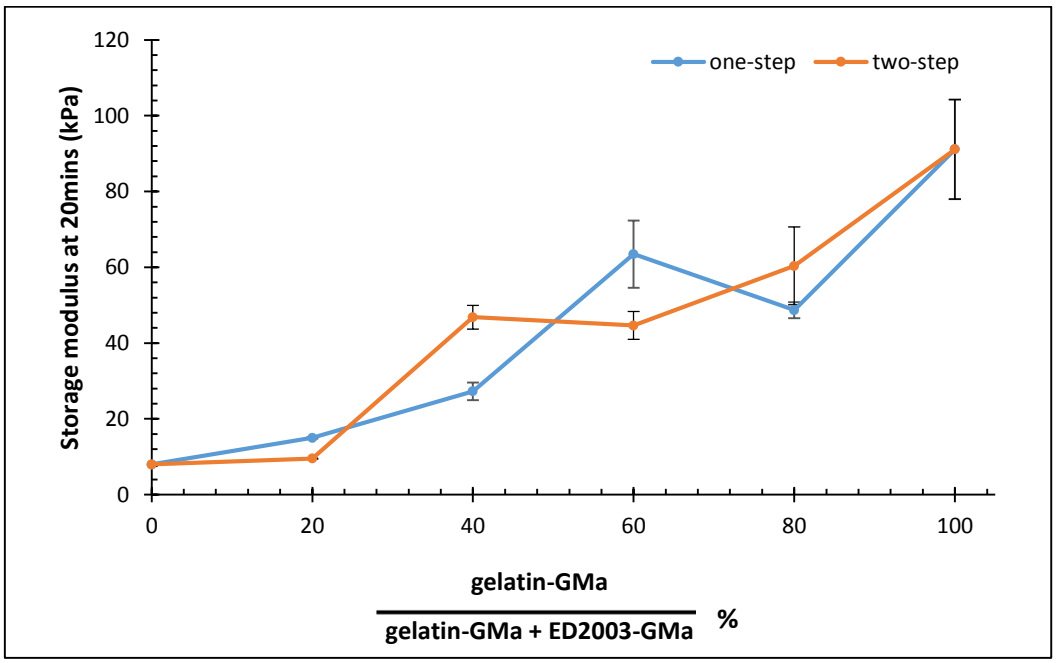

Figure 3.6: (a) Average storage modulus after 20 minutes of curing for gelatin-ED2003-MAh hydrogels with a TPC of 20% at 40°C and (b) average storage modulus after 20 minutes of curing for gelatin-ED2003-GMa hydrogels with a TPC of 20% at 40°C.

3.4. Compression testing

Compression testing was undertaken to compare the mechanical characteristics of varying ratios of gelatin-ED2003-methacrylated hydrogels prepared using one-step and two-step synthesis with either GMa or MAh. Stress-strain curves for four hydrogel products with a TPC of 20% were produced (Fig 3.7). All curves were found to have a standard 'J-shaped' configuration.

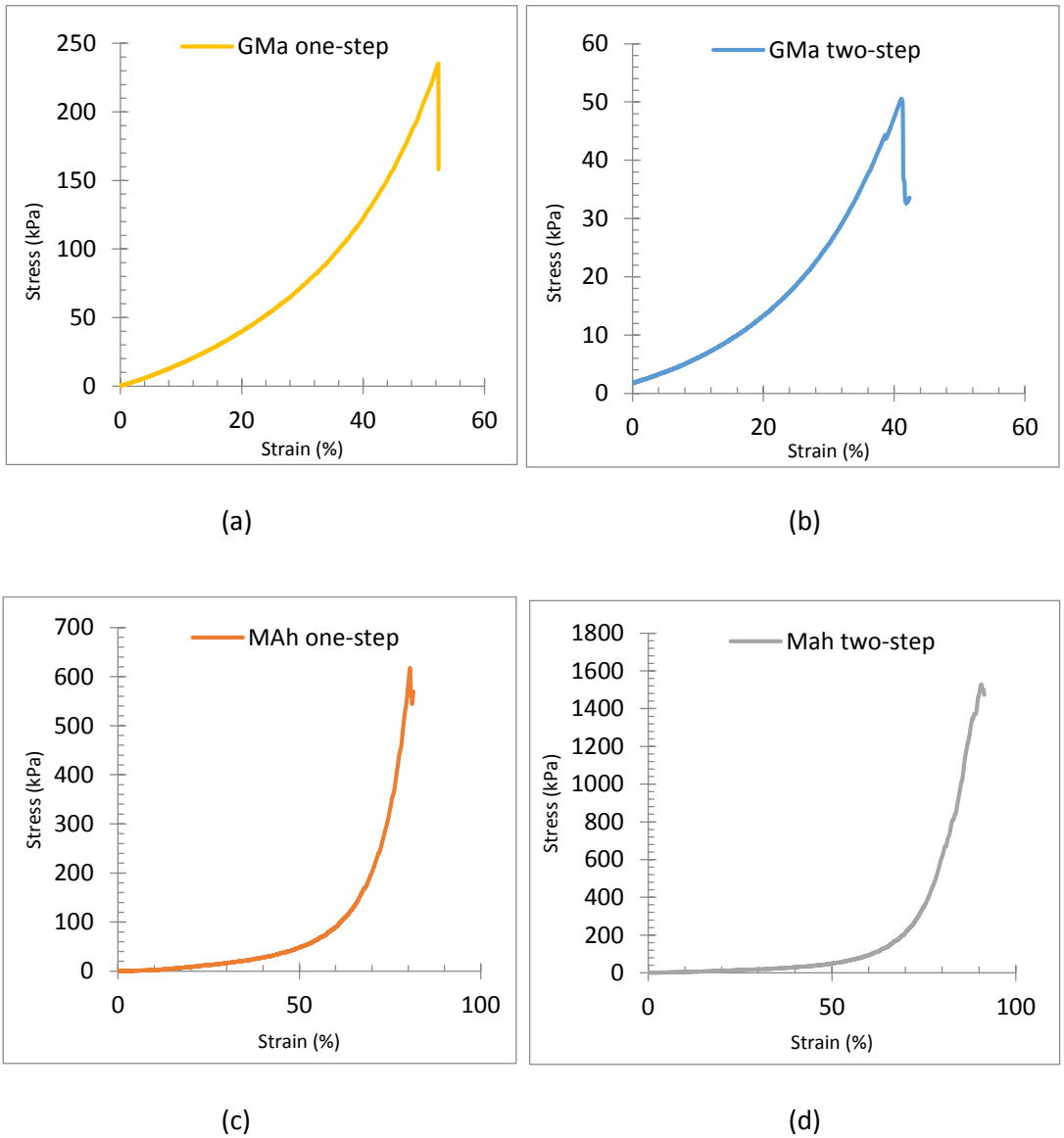

Figure 3.7: Stress-strain curves of G(80%):E(20%) with a TPC of 20% and made with (a) GMa methacrylate by one-step synthesis, (b) GMa methacrylate by two-step synthesis, (c) MAh methacrylate by one-step synthesis and (d) MAh methacrylate by two-step synthesis.

Overall, MAh based hydrogels exhibit higher compressive stress values and work of fracture values than that of the GMa hydrogels, with maximum values recorded at σ_c = 2.5 ±0.2 MPa and W_c = 246 ±25 kJ/m^3 for G(90%):E(10%) MAh hydrogels produced by two-step synthesis. By comparing the synthesis methods using MAh, a significant increase in the robustness of two-step synthesis is noted in the G(80%-90%):E(20%-10%) region, compared with one-step synthesis (Fig 3.8 (a) and Fig 3.9 (a)). This increase may be due to residual unreacted methacrylic acid being present in the MAh based gels leading to polymethacrylic acid being present in the final product and giving additional elastic support to the hydrogels. However, generally the compressive stress results show that the toughest gels are those with gelatin-methacrylate amounts between 60% - 90% of the TPC, which supports the previously discussed rheology results (page 44).

The hydrogels methacrylated with GMa show lower compressive stress to failure and work to failure values then the individual networks with the exception of the G(80%):E(20%) hydrogel by one-step synthesis (Fig 3.8 (b) and Fig 3.9 (b)). These results are in line with the previously discussed rheology results and confirm that GMa is not an effective crosslinking reagent for these hydrogels.

Further characterisation tests were carried out by swell testing and tensile testing the materials to further investigate the mechanical properties of these hydrogels under tension.

(a)

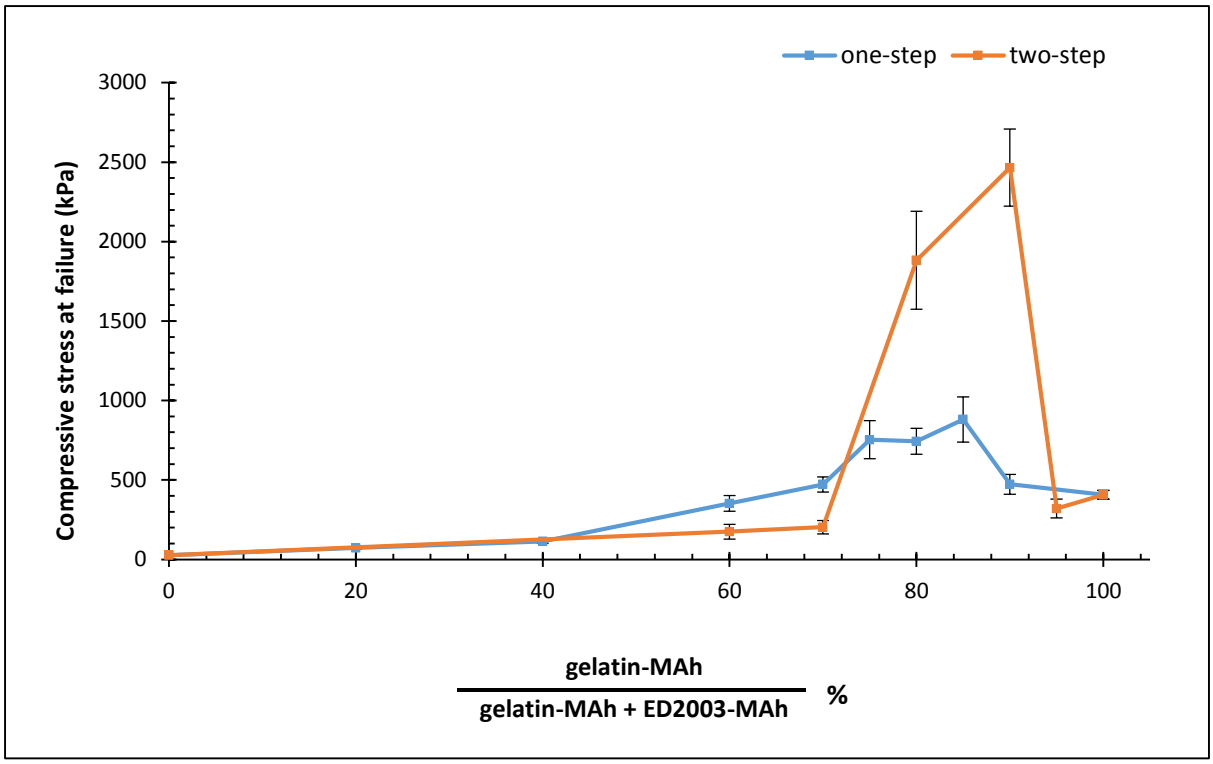

(b)

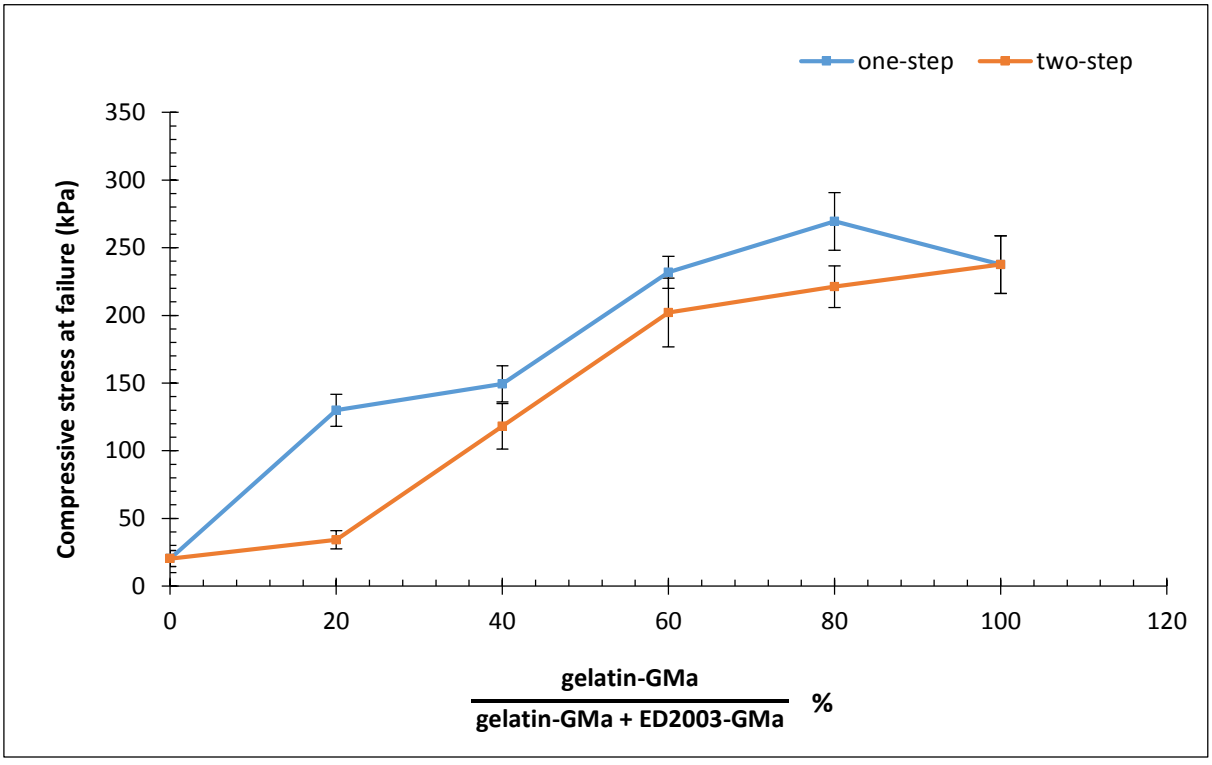

Figure 3.8: (a) Compressive stress at failure shown against the percentage of gelatin-MAh in the total polymer load for gelatin-ED2003-MAh hydrogels with a TPC of 20%. (b) Compressive stress at failure shown against the percentage of gelatin-GMa in the total polymer load for gelatin-ED2003-GMa hydrogels with a TPC of 20%.

(a)

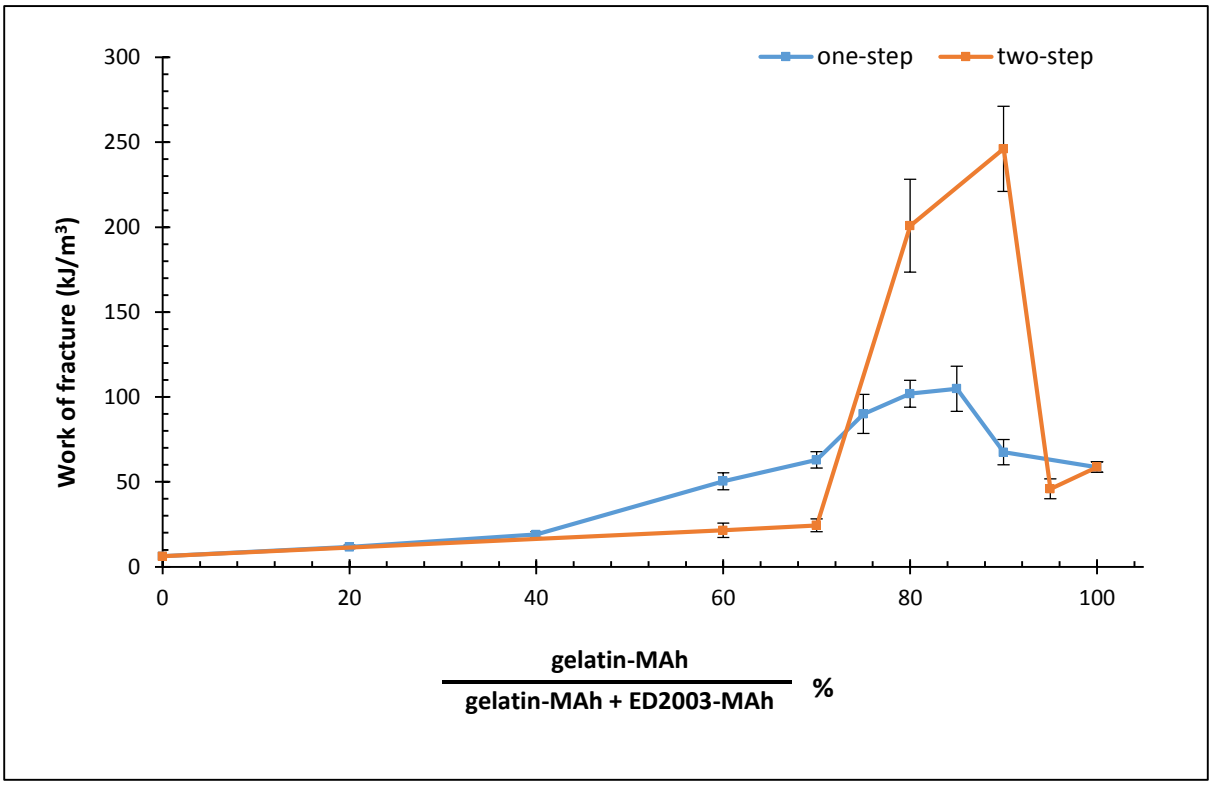

(b)

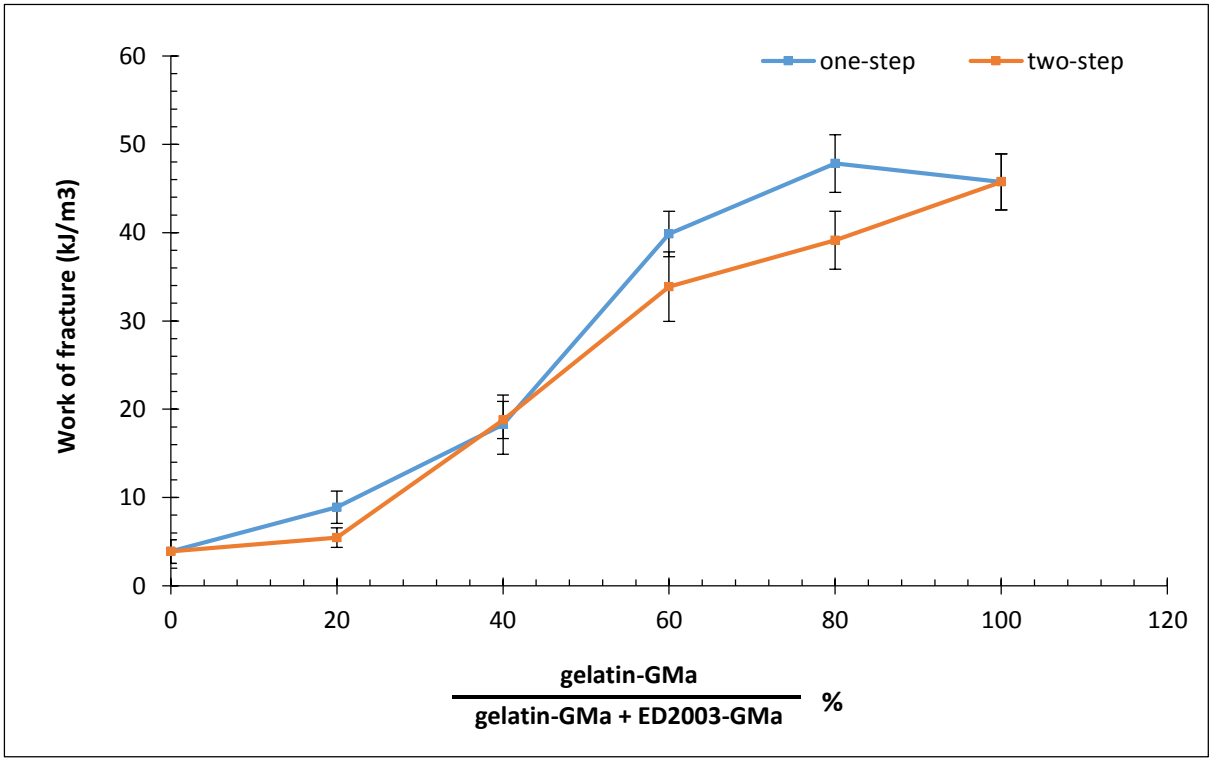

Figure 3.9: (a) Work to fracture shown against the percentage of gelatin-MAh in the total polymer load for gelatin-ED2003-MAh hydrogels with a TPC of 20%. (b) Work to fracture shown against the percentage of gelatin-GMa in the total polymer load for gelatin-ED2003-GMa hydrogels with a TPC of 20%.

3.5. Swelling Tests

Swelling tests were carried out on four hydrogels; G(80%):E(20%) with a TPC of 20%, produced by either one-step or two-step synthesis, and using with GMa or MAh as the respective methacrylate.

The swelling ratio and the equilibrium water content of the four hydrogel products was calculated using equation 7 and equation 8 (Table 3.3). The hydrogels with the greatest swelling ability were produced using the two-step method with MAh as the crosslinking reagent, while the hydrogels with the lowest swelling ability were one-step GMa hydrogels. This is consistent with the previously discussed crosslinking characteristic for both methacrylates. The two-step hydrogels have a higher swelling ratio than the one-step which indicates that the two-step method is creating two separate crosslinking reactions rather than increasing the crosslink density. This supports the suggestion that hydrogels prepared using the two-step synthesis contain a major double network and a minor single network.

Table 3.3: Swelling ratio (SR) and equilibrium water content (EWC) of G(80%):E(20%) hydrogels by either one-step or two-step synthesis with either MAh or GMa. Hydrogels were swollen in Milli-Q for 72 hours and then dried at 60^{o}C for 72 hours.

	dried	**swollen**	**SR**	**EWC**
	(g)	(g)		(%)
one-step w/GMa	0.43	2.75	6	84
two-step w/GMa	0.45	3.07	7	85
one-step w/MAh	0.35	7.08	20	95
two-step w/MAh	0.27	7.26	27	96

From observation, the hydrogels containing GMa were able to hold their structure better than the MAh based hydrogels (Fig 3.10). This suggests the GMa hydrogels may have a higher modulus range, meaning their cross-links are more compact and able to take less strain hence these gels are more likely to keep the hydrogel structure intact. The MAh hydrogels may have a higher modulus,

meaning their cross-links are more flexible and more likely to deform the hydrogel as seen in Fig 3.10.

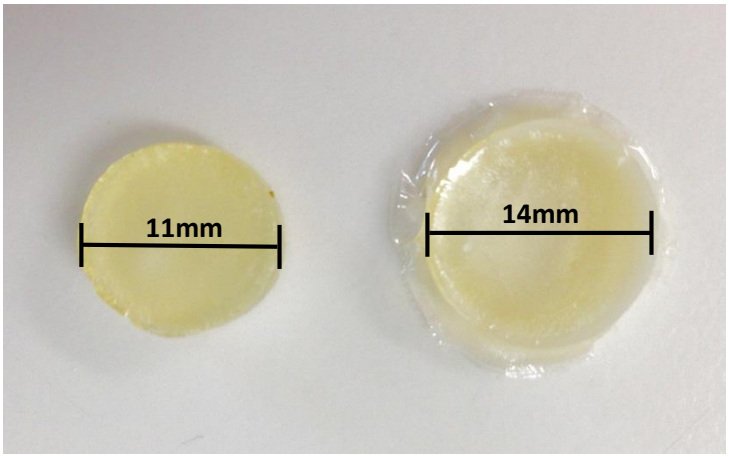

Figure 3.10: The results of dehydration on G(80%):E(20%) hydrogels produced by one-step synthesis with a TPC of 20%, and GMa methacrylate (left), MAh methacrylate (right)

As absorbance is one of the main properties of a hydrogel, compression testing was undertaken on G(80%):E(20%) by two-step synthesis with MAh as the curing agent swollen in Milli-Q for 72 hours (Table 3.4). A substantial reduction in mechanical strength was observed in comparison to the non-swollen gels. This same results is seen throughout literature and is expected for these hydrogels.

Table 3.4: Compressive stress at failure (σ_c), compressive strain at failure (ε_c), work of fracture (W_c), and elastic modulus (E_c) of G(80%):E(20%) MAh hydrogels prepared by two-step synthesis. As-prepared gels were placed in 50ml Milli-Q for 72 hours at approximately 21°C.

	σ_c	ε_c	W_c	E_c
	(kPa)	(%)	(kJ/m^3)	(kPa)
Non swollen gels	1882 ±308	95 ±3	201 ±27	77 ±5
Swollen for 72 hrs	17 ±1	51 ±1	3 ±0.24	21 ±1

From the rheology, compression, and swelling results, it can be concluded that MAh is the optimum crosslinking agent for these hydrogels. Tensile testing was conducted on these hydrogels to gain a further understanding of the hydrogel characteristics.

3.6. Tensile testing

Tensile testing was performed on varying ratios of gelatin-ED2003-MAh hydrogels using both one-step and two-step syntheses. This range of testing specifically looked at the G(60%-90%):E(40%-10%) region as previous testing showed these to be the optimum region. The stress-strain curves seen in Fig 3.11 represent the elastic region in each of the listed hydrogel. The results vary in both strain and stress, which shows that both the synthesis method has a large influence on the hydrogel product.

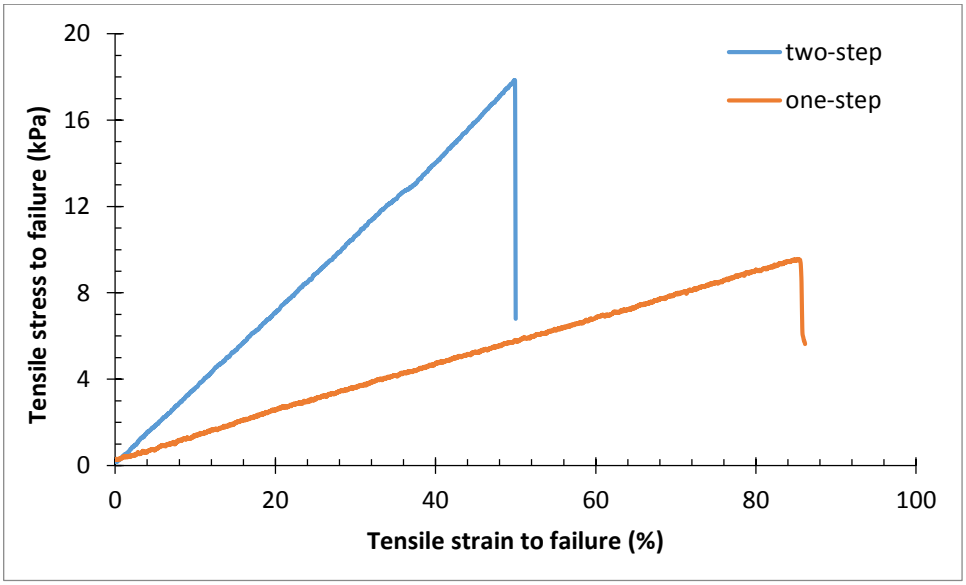

Figure 3.11: An example of the tensile stress-strain curve of G(80%):E(20%) MAh hydrogels by either one-step or two-step method.

The most elastic hydrogel is produced by one-step synthesis. As previously discussed, one-step synthesis is difficult to reproduce, and when using MAh there is the possibility that methacrylic acid is remaining in the final product resulting in this elastic property. This theory would also explain the lack of elasticity in the two-step MAh hydrogel in comparison to the one-step gel.

Testing of these hydrogels show that the two-step method produces robust but less elastic hydrogels (Fig 3.12). In contrast, the one-step method produces hydrogels that are mechanically weaker but have more elasticity (Fig 3.12). The mechanical characteristics of one-step hydrogel are similar to those of a gelatin single network hydrogel. As the gelatin and ED2003 are being methacrylated in the same vessel, the two polymers may be crosslinked by the methacrylate to create a solution with a major single network and minor gelatin-ED2003 double network. This is in contrast to the two-step method where polymers are methacrylate separately which is more likely to produce a double network gel.

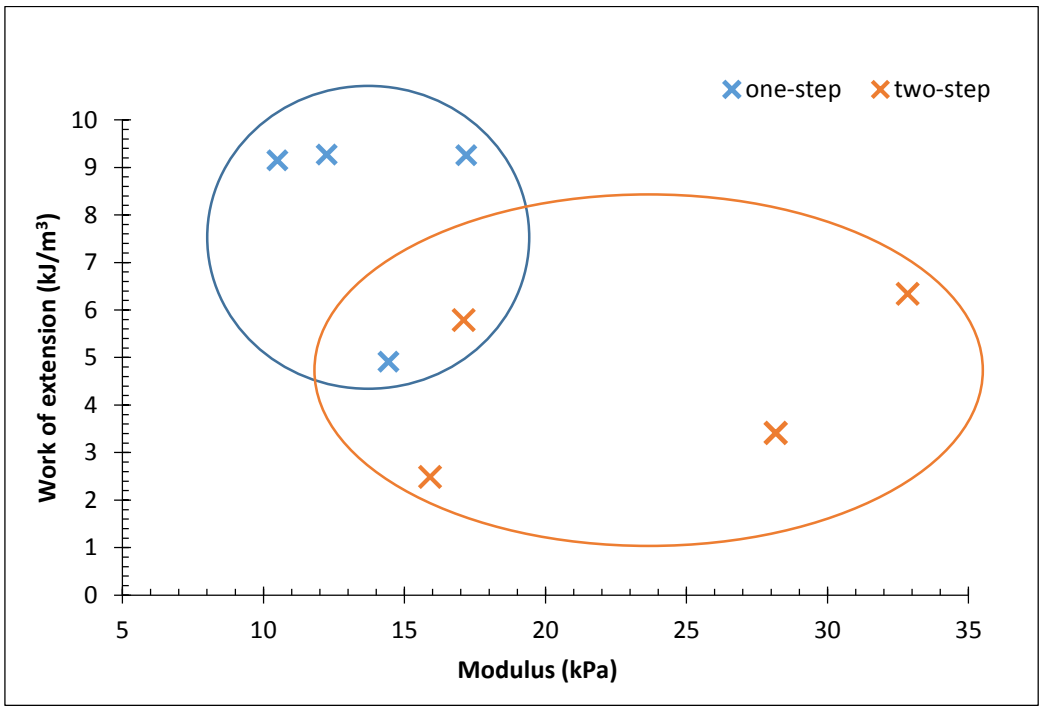

Figure 3.12: Modulus vs work of extension for G(80%):E(20%) MAh hydrogels with a TPC of 20%.

The tensile results also provide a more comprehensive view of the optimised gelatin-MA to ED2003-MA ratio in the TPC. Fig 3.13 shows a maximum tensile stress at failure, tensile strain at failure, work of fracture, and elastic modulus for G(70%):E(30%) MAh produced by two-step synthesis.

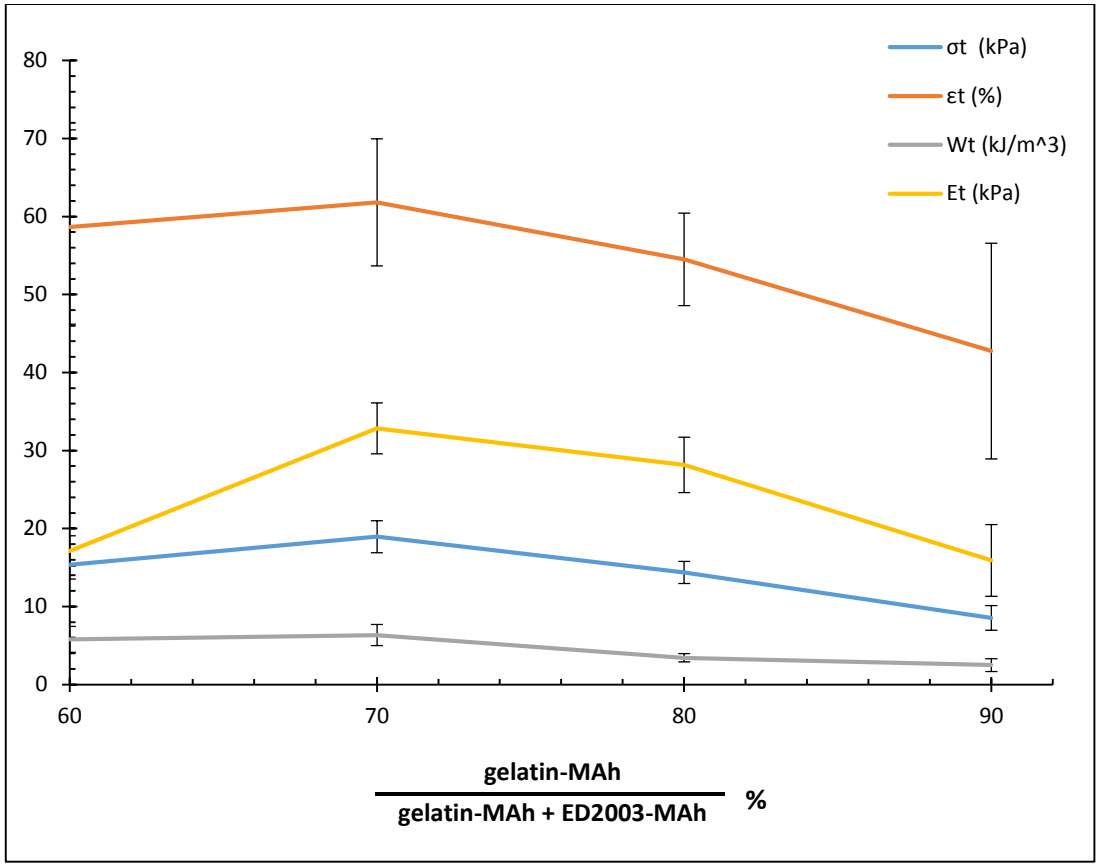

Figure 3.13: Tensile stress at failure (σ_t), tensile strain at failure (ε_t), work of fracture (W_t), and elastic modulus (E_t) of gelatin-ED2003-MAh hydrogels prepared by two-step synthesis for varying polymer ratios.

3.7. 3D printing

From the above results it can be concluded that G(80%):E(20%) MAh produced using two-step synthesis can create a mechanically robust hydrogel. The following tests will determine if this hydrogel can be extrusion printed.

Initial rheological measurements were performed on the uncured hydrogel solution to determine the solutions change in viscosity over a variable shear rate. The flow curve in Fig. 3.14 shows the flow properties of this material. These results were fitted to the power law model (equation 9) which calculated n = 0.14 ±0.002 and K = 500 ±5 Pa.s^n hence the solution is typical of a pseudo-plastic (non-Newtonian) fluid.

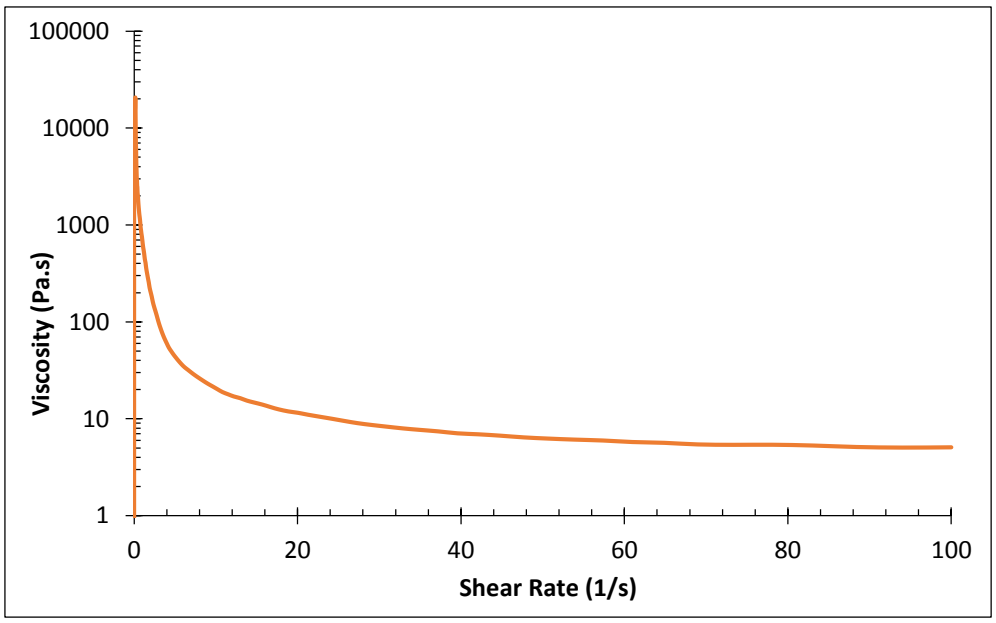

Figure 3.14: Flow curve of G(80%):E(20%) MAh produced using a two-step method.

The hydrogel solution was placed in a syringe and allowed to cool for approximately 5 minutes at 21^{o}C prior to being printed in the extrusion printer (Fig 3.15). As this solution contains gelatin, the mix entangled below 37^{o}C which increases the viscosity of the solution. This increase in viscosity was

noted by the increase in force required to extrude a constant amount of solution from the syringe over a 10 minute period; consisting of the time from when the solution is initially removed from the oven (60°C) to when the solution cools to room temperature (approx. 21°C). This property of gelatin gave the individually printed layers the structural integrity to allow for multiple layers of ink to be printed on top of one another before any curing is necessary (Fig 3.16 (a)). This is unlike any current printing methods where curing is required after each layer is printed.[26–28,81]

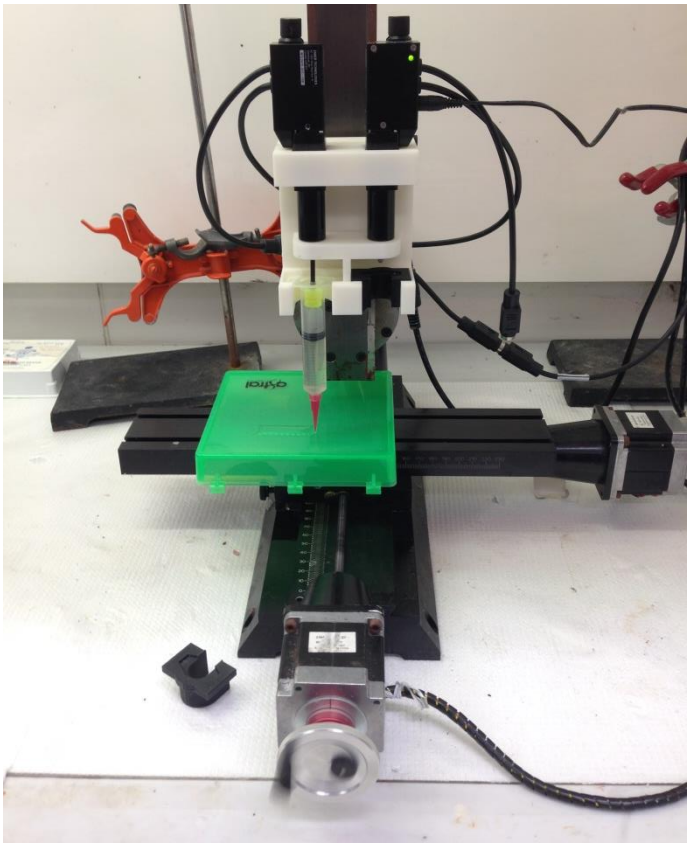

Figure 3.15: Image of the extrusion printer used in this study.

This method also allowed for permanent chemical crosslinks to form between the individual layers of the structure post printing (Fig 3.16). In current printing methods the individual layers are chemically cured after each layer is printed which restricts the amount crosslinking that can develop between the individual layers. As the entanglement is a reversible link, this restriction does not

occur in the method being discussed. The as-printed gels were mechanically tested and compared with the gels produced by casting to investigate the potential increases in mechanical strength by this method.

The printed structures where tested using tensile methods on a mechanical analyser. The results were compared with previous tensile tests on the same casted hydrogels (Fig. 3.17). It can be seen that there is no significant different in the results between the casted and as-printed hydrogels by either tensile stress at failure, tensile strain at failure, work of fracture, or elastic modulus. To the best of our knowledge, this result has not been seen in any currently available printing methods. [26–28,81]

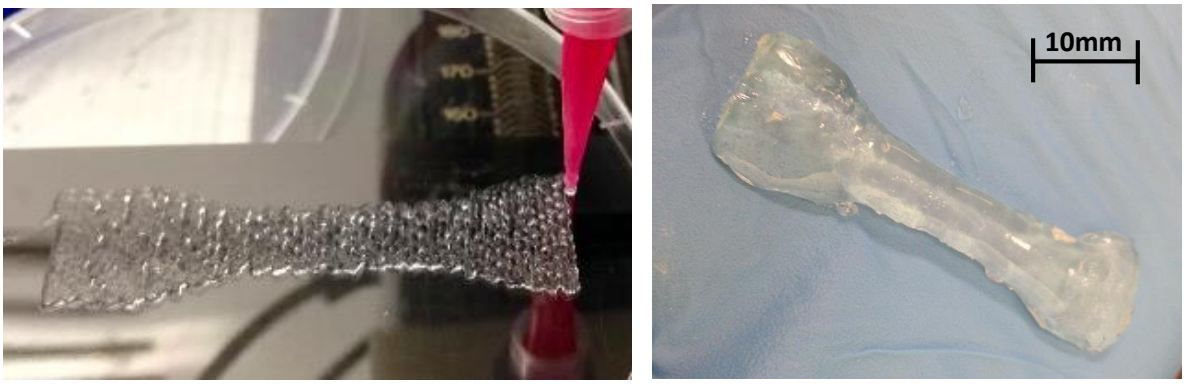

(a) (b)

Figure 3.16: (a) example of the first layer of a 3D printed dog bone and (b) example of a fully printed and cured dog bone

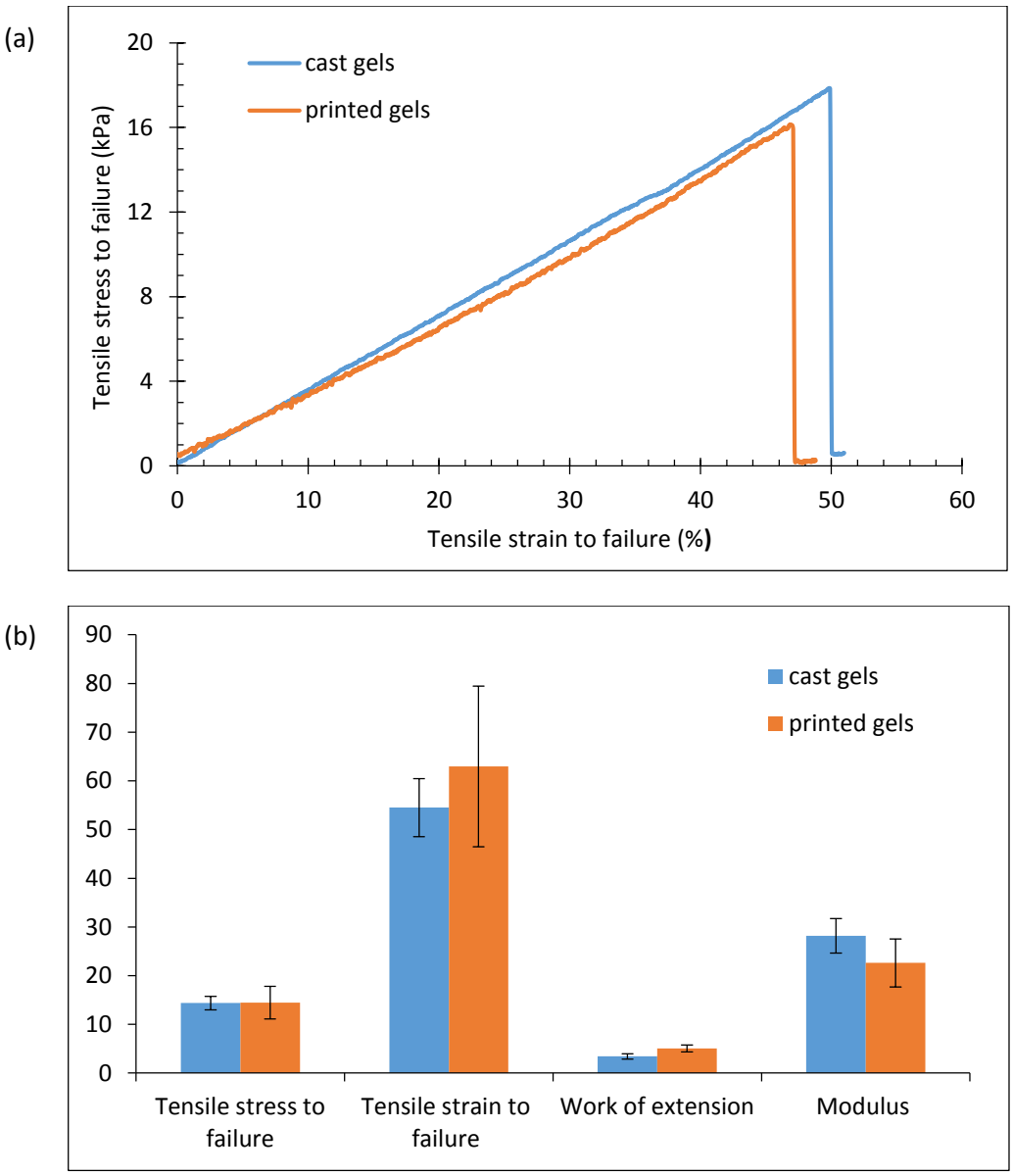

Figure 3.17: Comparison of casted and printed methods of G(80%):E(20%) MAh produced by two-step synthesis with a TPC of 20% by (a) stress-strain curves and (b) tensile testing data.

4. Conclusion

Hydrogels are increasingly being implemented as materials in modern technology and manufacturing applications due to their flexibility, biodegradability, and capability to respond to environmental factors. However, their wider use is being limited by their lack of mechanical robustness and their process-ability using additive manufacturing (3D printing). For example, although double network hydrogels are mechanically robust, it is not straightforward to 3D print these gels.

The main aim of this study was to synthesis and characterise a new mechanically robust double network gelatin – epoxy amine hydrogel that is 3D printable. The success of the study was measured against two key points; an improvement of the mechanical properties of the double network gel when compared to the individual polymer networks (showing clear results of optimisation or double network behaviour), and by successfully 3D printing hydrogels with mechanical characteristics similar to hydrogels prepared by casting.

Hydrogels were produced by combining methacrylated gelatin with methacrylated Jeffamine® ED2003 and using a curing agent to initiate photopolymerisation in the presence of UV light.

Four different curing agents were evaluated. Through rheological testing using a one-step synthesis method, it was found that Diphenyl(2,4,6-trimethylbenzoyl)phosphine oxide produced hydrogels with the highest storage modulus. Two different methacrylates were tested as potential crosslinking agents for both one-step and two-step synthesised hydrogels; methacrylic anhydride (MAh) and glycidyl methacrylate (GMa). Both rheology and compression testing showed that the hydrogels produced using MAh as the cross-linker formed mechanically robust products in comparison to their individual polymers unlike GMa.

Two different one-pot synthesis methods (one-step and two-step) were examined for their effectiveness to produce double network hydrogels with robust mechanical properties. The two-step synthesis method methacrylated the gelatin and ED2003 separately before combining them and adding the curing agent. The one-step method methacrylated both polymers concurrently in the same vessel and then added the curing agent. Rheology and compression testing revealed that gels prepared using the two-step method exhibited double network behaviour, whereas the one-step method did not produce mechanically robust gels.

The total polymer content (TPC) of the proposed hydrogels was optimised through rheological testing. Although the highest storage moduli were recorded by 25% gelatin-methacrylate and 40% ED2003-methacrylate, the reproducibility of these hydrogels was challenging due to their high viscosity. The optimised TPC for a reproducible hydrogel product was taken as 20%.

The ratio of gelatin-methacrylate to ED2003-methacrylate in the 20% TPC was optimised through rheology, compression and tensile testing. Rheology testing showed a significant increase in storage modulus for gels with a G(60%):E(40%) to G(90%):E(10%) ratio in the TPC (average G_{max} at 20 min for G(60%):E(40%) MAh by two-step synthesis = 168 ±27 kPa). Compression testing shows an increase in both compressive stress to failure (σ_c) and compressive strain energy to fracture (W_C) of between G(75%-90%):E(25%-10%) in the TPC. For example, compression testing of G(90%):E(10%) with MAh by two-step synthesis (80% water content) gives the result, σ_c = 2.5 ±0.2 MPa and W_C = 246 ±25 kJ/m^3, an 83% and 76% increase over the gelatin methacrylate lone polymer networks respectively. These results show an increase in robustness compared with similar structured gelatin based hydrogels found in literature.[57,85–87] However, as absorbance is one of the main properties of a hydrogel, the optimised gels were swollen in water for 72 hours post curing. Compression testing of these swollen hydrogels (96% water content) resulted in a significant loss in mechanical robustness

(G(80%):E(20%) MAh produced by two-step synthesis; σ_c = 17 ±1 kPa and W_C = 3.0 ±0.2 kJ/m^3). This effect is well known and expected. Tensile testing shows an increase in tensile stress at failure, tensile strain at failure, work of fracture, and elastic modulus of G(70%):E(30%) MAh hydrogels prepared by two-step synthesis with σ_t = 19 ±1 kPa and W_t = 6 ± 1 kJ/m^3.

Tensile testing was undertaken on hydrogels made with MAh by both one-step and two-step synthesis. Hydrogels prepared using the one-step method did not show much dependence on polymer ratio and produced robust hydrogels with poor elasticity. However, the two-step method showed an increase in elasticity as the percentage of gelatin increased, but they did not show much variation in strength. These two-step hydrogels exhibited a higher elasticity than the one-step gels. Tensile testing of these hydrogels show reduced tensile values against comparable double network hydrogels in current literature.[28,57,88,89]

The shear properties of the optimised hydrogel solution were tested using rheology and were fitted to the power law model to show the solution has non-Newtonian shear thinning properties. A new printing method was implemented where the gelatin contained in the solution was held at approximately 21°C for 5 mins prior to printing. This allowed for entanglement of the polymer network which increased the viscosity and gave structural integrity to the individual printed layers without the necessity to UV cure the gel between layers. This is unlike any current printing methods where curing is required after each layer is printed to create a structurally sound grounding for the following layer.[21,28,81,82,90] This printing method also allows the individual layers of the printed gel to crosslink with each other. Again, this has not be seen in other printing methods where the first layer is often fully cued before coming into contact with any sequential layers. This accessibility to chemically crosslink in all three dimensions resulted in as-printed gels with similar properties to the same casted materials.

The as-printed hydrogel samples were tensile tested and compared with cast hydrogel samples. The printed samples do not show any significant reduction in tensile stress or work of extension in comparison to the cast samples. To the best of our knowledge, this is the first demonstration of 3D printed gels without significant loss in mechanical strength (compared to cast gels).

Concluding, a new mechanically robust double network hydrogel was developed, characterised, and shown to be capable of extrusion printing. Noticeably, a new method of extrusion printing was developed to allow gels to be extrusion printed while maintaining their mechanical robustness.

4.1. Future work

This study revealed that the chemistry of these gel materials is highly complex. The structural chemistry of both the one-step and two-step synthesis hydrogels were analysed by NMR spectroscopy. The two–pot method spectrum contains the individual signals of the two polymers as well as clear signs of methacrylation and crosslinking. The one-step method spectrum is much more complicated and it is difficult to decipher without further analyses. During the two-step method, the ED2003 and gelatin are methacrylated separately so no cross methacrylation can occur, resulting in a purer double network structure that would have a more defined NMR structure. During the one-step synthesis, both polymers are methacrylated together which is thought to lead to a single interlinked network system. Due to the multiple functional groups on each of the two polymer networks, the chemistry in this second method has a much large variety of possible reactions which would lead to its complicated NMR spectrum with broad peaks. It is recommend that further investigation is undertaken to fully understanding the chemistry of these hydrogels. This may include investigating what reactions can possibly take place and the theorised precedence of these reactions. A higher level NMR analyses (600-900 MHz system) or fluorescent tagging could also help with clarification of the final structure.

Additional study could be undertaken to characterise the hydrogel product in different environments or using other chemicals. Some examples are as follows; researching and testing additional types of photoinitiators and crosslinkers, running the experiments at different temperatures and humidity, and investigating the effects of pH on the synthesis process.

It may also be possible to further increase the mechanical robustness of these hydrogel by reinforcing them with fibres or similar materials. Previous studies using a variety of hydrogels have indicated that the addition of reinforcing fillers that can absorb or dissipate mechanical energy result in improved mechanical strength.[91] Fibres can be inserted in to the gels through many different techniques including weaving or knitting, printing, or developing a fibre from a polymer network that can then be absorbed into a second network.[92–94]

As previously mentioned, it was also noted during compression testing that cured hydrogels with a higher percentage of gelatin methacrylate were seen to contain their water more effectively. It would be recommend to repeat the swell testing with varying ratios of gelatin-MA to ED2003-MA to identify the effect each polymer has on the swelling ability of the hydrogels.

The ability of these hydrogel to be cured post printing also opens up the possibility of further study into applications for methacrylated hydrogels such as wound dressings or surgical implants that can be printed into a specific form directly into the required area before being cured.

5. References

1. Rosiak, J. M. & Yoshii, F. Hydrogels and their medical applications. *Nucl. Instruments Methods Phys. Res. B* **151,** 56–64 (1999).
2. Zohuriaan-Mehr, M. J., Omidian, H., Doroudiani, S. & Kabiri, K. Advances in non-hygienic applications of superabsorbent hydrogel materials. *J. Mater. Sci.* **45,** 5711–5735 (2010).
3. Inganäs, O. & Ghosh, S. Conducting Polymer Hydrogels as 3D Electrodes : Applications for Supercapacitors. *Adv. Mater.* **11,** 1214–1218 (1999).
4. Buwalda, S. J., Boere, K. W. M., Dijkstra, P. J., Feijen, J., Vermonden, T. & Hennink, W. E. Hydrogels in a historical perspective: From simple networks to smart materials. *J. Control. Release* **190,** 254–273 (2014).
5. Naficy, S., Razal, J. M., Spinks, G. M., Wallace, G. G. & Whitten, P. G. Electrically conductive, tough hydrogels with pH sensitivity. *Chem. Mater.* **24,** 3425–3433 (2012).
6. Yu, C., Duan, Z., Yuan, P., Li, Y., Su, Y., Zhang, X., Pan, Y., Dai, L. L., Nuzzo, R. G., Huang, Y., Jiang, H. & Rogers, J. a. Electronically programmable, reversible shape change in two- and three-dimensional hydrogel structures. *Adv. Mater.* **25,** 1541–1546 (2013).
7. Keplinger, C., Sun, J.-Y., Foo, C. C., Rothemund, P., Whitesides, G. M. & Suo, Z. Stretchable, Transparent, Ionic Conductors. *Science* **341,** 984–987 (2013).
8. Chun-lei, J. & Tangkai. A Temperature-sensitive hydrogel for suppressing oil Fire. *Adv. Mater. Res. Vols* **785-786,** 724–728 (2013).
9. Yang, Y., Deng, J., Zhao, D. & Guo, J. Mechanism and Property of Extinguishing Temperature-sensitive Hydrogels. in *2014 7th International Conference on Intelligent Computation Technology and Automation* 360–364 (2014). doi:10.1109/ICICTA.2014.94
10. Rudzinski, W. E., Dave, A. M., Vaishnav, U. H., Kumbar, S. G., Kulkarni, A. R. & Aminabhavi, T. M. Designed Monomers and Polymers Hydrogels as controlled release devices in agriculture. *Des. Monomers Polym.* **5,** 39–65 (2002).

11. Koo, H.-J. & Velev, O. D. *Regenerable photovoltaic devices with a hydrogel-embedded microvascular network. Scientific reports* **3,** (2013).

12. Landers, R., Hubner, U., Schmelzeisen, R. & Mulhaupt, R. Rapid prototyping of scaffolds derived from thermoreversible hydrogels and tailored for applications in tissue engineering. *Biomaterials* **23,** 4437–4447 (2002).

13. Gore, J. C., Brown, M. S., Zhong, J., Mueller, K. F. & Good, W. NMR relaxation of water in hydrogel polymers: a model for tissue. *Magn. Reson. Med.* **9,** 325–332 (1989).

14. Camci-Unal, G., Annabi, N., Dokmeci, M. R., Liao, R. & Khademhosseini, A. Hydrogels for cardiac tissue engineering. *NPG Asia Mater.* **6,** e99 (2014).

15. Caló, E. & Khutoryanskiy, V. V. Biomedical applications of hydrogels: A review of patents and commercial products. *Eur. Polym. J.* **65,** 252–267 (2015).

16. Sun, J.-Y., Zhao, X., Illeperuma, W. R. K., Chaudhuri, O., Oh, K. H., Mooney, D. J., Vlassak, J. J. & Suo, Z. Highly stretchable and tough hydrogels. *Nature* **489,** 133–136 (2012).

17. Gong, J. P., Katsuyama, Y., Kurokawa, T. & Osada, Y. Double-Network Hydrogels with Extremely High Mechanical Strength. *Adv. Mater.* **15,** 1155–1158 (2003).

18. Kirchmajer, D. M. & in het Panhuis, M. Reinforcing biopolymer hydrogels with ionic-covalent entanglement hydrogel microspheres. *J. Appl. Polym. Sci.* **131,** (2014).

19. Lipson, H. & Kurman, M. *Fabricated: The New World of 3D Printing*. (Wiley, 2013).

20. Jones, N. Science in three dimensions: The print revolution. *Nature* **487,** 22–23 (2012).

21. Billiet, T., Vandenhaute, M., Schelfhout, J., Van Vlierberghe, S. & Dubruel, P. A review of trends and limitations in hydrogel-rapid prototyping for tissue engineering. *Biomaterials* **33,** 6020–6041 (2012).

22. Yan, X. & Gu, P. A review of rapid prototyping technologies and systems. *CAD Comput. Aided Des.* **28,** 307–318 (1996).

23. Calvert, P. & Zengshe, L. Freeform fabrication of hydrogels. *Acta Materialia* **46,** 2565–2571 (1998).

24. Lipson, H. & Kurman, M. *Fabricated: The new world of 3D printing.* (John Wiley & Sons, 2013).

25. Duan, B., Hockaday, L. A., Kang, K. H. & Butcher, J. T. 3D Bioprinting of heterogeneous aortic valve conduits with alginate/gelatin hydrogels. *J. Biomed. Mater. Res. - Part A* **101A,** 1255–1264 (2013).

26. Bakarich, S. E., Gorkin III, R., in het Panhuis, M. & Spinks, G. M. Three-Dimensional Printing Fiber Reinforced Hydrogel Composites. *ACS Appl. Mater. Interfaces* **6,** 15998–16006 (2014).

27. Bakarich, S. E., Balding, P., Gorkin III, R., Spinks, G. M. & in het Panhuis, M. Printed ionic-covalent entanglement hydrogels from carrageenan and an epoxy amine. *RSC Adv.* **4,** 38088–38092 (2014).

28. Bakarich, S. E., in het Panhuis, M., Beirne, S., Wallace, G. & Spinks, M. Extrusion printing of ionic – covalent entanglement hydrogels with high toughness. *J. Mater. Chem. B* **1,** 4939–4946 (2013).

29. Peppas, N. a. & Khare, A. R. Preparation, structure and diffusional behavior of hydrogels in controlled release. *Adv. Drug Deliv. Rev.* **11,** 1–35 (1993).

30. Horkay, F., Tasaki, I. & Basser, P. J. Effect of monovalent-divalent cation exchange on the swelling of polyacrylate hydrogels in physiological salt solutions. *Biomacromolecules* **2,** 195–199 (2001).

31. Kamata, H., Akagi, Y., Kayasuga-Kariya, Y., Chung, U. & Sakai, T. “Nonswellable” hydrogel without mechanical hysteresis. *Science* **343,** 873–875 (2014).

32. Eliyahu-Gross, S. & Bitton, R. Environmentally responsive hydrogels with dynamically tunable properties as extracellular matrix mimetic. *Rev. Chem. Eng.* **29,** 159–168 (2013).

33. Anseth, K. S., Bowman, C. N. & Brannon-Peppas, L. Mechanical properties of hydrogels and their experimental determination. *Biomaterials* **17,** 1647–1657 (1996).

34. Qiu, L. Y. & Bae, Y. H. Polymer architecture and drug delivery. *Pharm. Res.* **23,** 1–30 (2006).

35. Angelova, N. & Hunkeler, D. Rationalizing the design of polymeric biomaterials. *Trends Biotechnol.* **17,** 409–421 (1999).

36. Barner-Kowollik, C. & Inglis, A. J. Has click chemistry lead to a paradigm shift in polymer material design? *Macromol. Chem. Phys.* **210,** 987–992 (2009).

37. Gibas, I. & Janik, H. Review : Synthetic Polymer Hydrogels for Biomedical. *Chem. Technol.* **4,** 297–304 (2010).

38. Rubinstein, M. & Colby, R. H. *Polymer Physics*. (Oxford University Press, 2003).

39. Dorset, D., Strauss, H. L. & Snyder, R. G. Chain-length dependence of the melting point difference between hydrogenated and deuterated crystalline n-alkanes. *J. Phys. Chem.* **95,** 938–940 (1991).

40. Graessley, W. W. Effect of long branches on the flow properties of polymers. *Acc. Chem. Res.* **10,** 332–339 (1977).

41. Fréchet, J. M. J. Functional polymers and dendrimers: reactivity, molecular architecture, and interfacial energy. *Science* **263,** 1710–1715 (1994).

42. Torres, J. M., Wang, C., Coughlin, E. B., Bishop, J. P., Register, R. a, Riggleman, R. a, Stafford, C. M. & Vogt, B. D. Influence of chain stiffness on thermal and mechanical properties of polymer thin films. *Macromolecules* **44,** 9040–9045 (2011).

43. Mattson, G., Conklin, E., Desai, S., Nielander, G., Savage, M. D. & Morgensen, S. A practical approach to crosslinking. *Mol. Biol. Rep.* **17,** 167–183 (1993).

44. Nguyen, K. T. & West, J. L. Photopolymerizable hydrogels for tissue engineering applications. *Biomaterials* **23,** 4307–4314 (2002).

45. Scranton, A. B., Bowman, C. N. & Peiffer, R. W. *Photopolymerization*. *ACS Symposium Series* **673,** (1997).

46. Allen, N. S. Photoinitiators for UV and visible curing of coatings: Mechanisms and properties. *J. Photochem. Photobiol. A Chem.* **100,** 101–107 (1996).

47. Okay, O. & Durmaz, S. Charge density dependence of elastic modulus of strong polyelectrolyte hydrogels. *Polymer* **43,** 1215–1221 (2002).

48. Horkay, F., Hecht, A. M. & Geissler, E. Effect of cross-links on the swelling equation of state: polyacrylamide hydrogels. *Macromolecules* **22,** 2007–2009 (1989).

49. Barbucci, R., Magnani, A. & Consumi, M. Swelling behavior of carboxymethylcellulose hydrogels in relation to crosslinking, pH, and charge density. *Macromolecules* **33,** 7475–7480 (2000).

50. Lee, K. Y., Rowley, J. a., Eiselt, P., Moy, E. M., Bouhadir, K. H. & Mooney, D. J. Controlling mechanical and swelling properties of alginate hydrogels independently by cross-linker type and crosslinking density. *Macromolecules* **33,** 4291–4294 (2000).

51. Bakarich, S. E., Pidcock, G. C., Balding, P., Stevens, L., Calvert, P. & in het Panhuis, M. Recovery from applied strain in interpenetrating polymer network hydrogels with ionic and covalent cross-links. *Soft Matter* **8,** 9985–9988 (2012).

52. Haque, M. A., Kurokawa, T. & Gong, J. P. Super tough double network hydrogels and their application as biomaterials. *Polymer* **53,** 1805–1822 (2012).

53. Sperling, L. H. in *Interpenetrating Polymer Networks* 3–38 (1994). doi:10.1163/092764410X490509

54. Na, Y. H. Double network hydrogels with extremely high toughness and their applications. *Korea-Australia Rheol. J.* **25,** 185–196 (2013).

55. Dragan, E. S. Design and applications of interpenetrating polymer network hydrogels. A review. *Chem. Eng. J.* **243,** 572–590 (2014).

56. Gong, J. P. Why are double network hydrogels so tough? *Soft Matter* **6,** 2583–2590 (2010).

57. Kirchmajer, D. M. & in het Panhuis, M. Robust biopolymer based ionic–covalent entanglement hydrogels with reversible mechanical behaviour. *J. Mater. Chem. B* **2,** 4694–4702 (2014).

58. Martin, J. E. & Adolf, D. The Sol-Gel Transition In Chemical Gels. *Annual Review of Physical Chemistry* **42,** 311–339 (1991).

59. Klein, L. . & Garvey, G. . Kinetics of the sol/gel transition. *Journal of Non-Crystalline Solids* **38-39,** 45–50 (1980).

60. Datasheet: Gelatin from porcine skin, Type A. *Sigma Aldrich, Australia*

61. Datasheet: Gelatin from bovine skin, Type B. *Sigma Aldrich, Australia*

62. U.S. Food and Drug Administration. http://www.fda.gov/Food/IngredientsPackagingLabeling/GRAS/SCOGS/ucm261307.htm.

63. Product Information: Gelatin. *Sigma Aldrich, Australia*

64. Djabourov, M., Leblond, J. & Papon, P. Gelation of aqueous gelatin solutions. II. Rheology of the sol-gel transition. *Journal de Physique* **49,** 333–343 (1988).

65. Bello, J., Bello, H. R. & Vinograd, J. R. The functional groups in the gelation of gelatin. *Biochim. Biophys. Acta* **57,** 222–229 (1962).

66. Kuwajlma, T., Yoshida, H. & Hayashi, K. Graft Polymerization of Methyl Methacrylate Onto Gelatin. *J. Appl. Polym. Sci.* **20,** 967–974 (1976).

67. Coimbra, P., Gil, M. H. & Figueiredo, M. Tailoring the properties of gelatin films for drug delivery applications: Influence of the chemical crosslinking method. *Int. J. Biol. Macromol.* **70,** 10–19 (2014).

68. Sivakumar, M., Rajalingam Ganga Radhakrishnan, P. & Kothandaraman, H. Grafting of glycidyl methacrylate onto gelatin. *J. Appl. Polym. Sci.* **43,** 1789–1794 (1991).

69. Topkaya, S. N. Gelatin methacrylate (GelMA) mediated electrochemical DNA biosensor for DNA hybridization. *Biosens. Bioelectron.* **64,** 456–461 (2015).

70. Van Den Bulcke, a I., Bogdanov, B., De Rooze, N., Schacht, E. H., Cornelissen, M. & Berghmans, H. Structural and rheological properties of methacrylamide modified gelatin hydrogels. *Biomacromolecules* **1,** 31–38 (2000).

71. Young, S., Wong, M., Tabata, Y. & Mikos, A. G. Gelatin as a delivery vehicle for the controlled release of bioactive molecules. *J. Control. Release* **109,** 256–274 (2005).

72. Rattanaruengsrikul, V., Pimpha, N. & Supaphol, P. In vitro efficacy and toxicology evaluation of silver nanoparticle-loaded gelatin hydrogel pads as antibacterial wound dressings. *J. Appl. Polym. Sci.* **124,** 1668–1682 (2012).

73. Lee, Y., Bae, J. W., Oh, D. H., Park, K. M., Chun, Y. W., Sung, H. J. & Park, K. D. In situ forming gelatin-based tissue adhesives and their phenolic content-driven properties. *J. Mater. Chem. B* **1,** 2407–2414 (2013).

74. Elvin, C. M., Vuocolo, T., Brownlee, A. G., Sando, L., Huson, M. G., Liyou, N. E., Stockwell, P. R., Lyons, R. E., Kim, M., Edwards, G. a., Johnson, G., McFarland, G. a., Ramshaw, J. a M. & Werkmeister, J. a. A highly elastic tissue sealant based on photopolymerised gelatin. *Biomaterials* **31,** 8323–8331 (2010).

75. The Jeffamine® Polyetheramines. *Huntsman* at <http://www.huntsman.com/portal/page/portal/performance_products/Media Library/global/files/jeffamine_polyetheramines.pdf>

76. Demir, K. D., Kiskan, B., Aydogan, B. & Yagci, Y. Thermally curable main-chain benzoxazine prepolymers via polycondensation route. *React. Funct. Polym.* **73,** 346–359 (2013).

77. The Jeffamine® Polyetheramines. *Huntsman* at <https://www.huntsmanservice.com/performance_products/Media Library/global/files/epoxy_formulations_using_Jeffamine? _polyetheramines.pdf>

78. Jeffamine® Polyetheramines. *Huntsman* at <http://www.alfa-chemicals.co.uk/Divisions/Industrial/Industrial-Products/Industrial-ProductGroupDetails.aspx?p=437&Product Group=JEFFAMINE? ◆+Polyetheramines>

79. Barnes, H. A., Hutton, J. F. & Walters, K. *An introduction to rheology*. (Elsevier, 1989).

80. Mezger, T. G. *The Rheology Handbook: For Users of Rotational and Oscillatory Rheometers*. (Vincentz Network GmbH & Co KG, 2006).

81. Kirchmajer, D. M., Gorkin, R. & in het Panhuis, M. An overview of the suitability of hydrogel forming polymers for extrusion-based 3D-printing. *J. Mater. Chem. B* **3,** 4105–4117 (2015).

82. Skardal, A., Zhang, J., McCoard, L., Xu, X., Oottamasathien, S. & Prestwich, G. D. Photocrosslinkable hyaluronan-gelatin hydrogels for two-step bioprinting. *Tissue Eng. Part A* **16,** 2675–2685 (2010).

83. Rattanakit, P., Moulton, S. E., Santiago, K. S., Liawruangrath, S. & Wallace, G. G. Extrusion printed polymer structures: A facile and versatile approach to tailored drug delivery platforms. *Int. J. Pharm.* **422,** 254–263 (2012).

84. Photoinitiators. *Sigma Aldrich, Australia* at <https://www.sigmaaldrich.com/content/dam/sigma-aldrich/docs/Aldrich/General_Information/photoinitiators.pdf>

85. Kirchmajer, D. M., Watson, C. A., Ranson, M. & in het Panhuis, M. Gelapin, a degradable genipin crosslinked gelatin hydrogel. *RSC Adv.* **3,** 1073–1081 (2013).

86. Xiao, W., He, J., Nichol, J. W., Wang, L., Hutson, C. B., Wang, B., Du, Y., Fan, H. & Khademhosseini, A. Synthesis and characterization of photocrosslinkable gelatin and silk fibroin interpenetrating polymer network hydrogels. *Acta Biomater.* **7,** 2384–2393 (2011).

87. Shin, H., Olsen, B. D. & Khademhosseini, A. The mechanical properties and cytotoxicity of cell-laden double-network hydrogels based on photocrosslinkable gelatin and gellan gum biomacromolecules. *Biomaterials* **33,** 3143–3152 (2012).

88. Naficy, S., Brown, H. R., Razal, J. M., Spinks, G. M. & Whitten, P. G. Progress Toward Robust Polymer Hydrogels. *Aust. J. Chem.* **64,** 1007–1025 (2011).

89. Hago, E. E. & Li, X. Interpenetrating polymer network hydrogels based on gelatin and PVA by biocompatible approaches: Synthesis and characterization. *Adv. Mater. Sci. Eng.* 1–8 (2013). doi:10.1155/2013/328763

90. Hockaday, L. a, Kang, K. H., Colangelo, N. W., Cheung, P. Y. C., Duan, B., Malone, E., Wu, J., Girardi, L. N., Bonassar, L. J., Lipson, H., Chu, C. C. & Butcher, J. T. Rapid 3D printing of anatomically accurate and mechanically heterogeneous aortic valve hydrogel scaffolds. *Biofabrication* **4,** 1–22 (2012).

91. Zhao, X. Multi-scale multi-mechanism design of tough hydrogels: building dissipation into stretchy networks. *Soft Matter* **10,** 672 (2014).

92. Agrawal, A., Rahbar, N. & Calvert, P. D. Strong fiber-reinforced hydrogel. *Acta Biomater.* **9,** 5313–5318 (2013).

93. Young, C. D., Wu, J. R. & Tsou, T. L. High-strength, ultra-thin and fiber-reinforced pHEMA artificial skin. *Biomaterials* **19,** 1745–1752 (1998).

94. Coburn, J., Gibson, M., Bandalini, P. A., Laird, C., Mao, H. Q., Moroni, L., Seliktar, D. & Elisseeff, J. Biomimetics of the extracellular matrix: An integrated three-dimensional fiber-hydrogel composite for cartilage tissue engineering. *Smart Struct. Syst.* **7,** 213–222 (2011).

1. Appendix 1 – Volume

Table A1.1: Material volumes required to produce Gelatin-MA with varying TPC.

% TPC	**Gelatin** (g)	**Methacrylate** (ml)	**Milli-Q** (ml)
30	12.50	2.40	35.00
25	10.42	2.00	37.50
20	8.33	1.60	40.00
15	6.25	1.20	42.50
10	4.17	0.80	45.00
5	2.08	0.40	47.50

Table A1.2: Material volumes required to produce ED2003-MA with varying TPC.

% TPC	**ED2003** (ml)	**Glycidyl Methacrylate** (ml)	**Milli-Q** (ml)
50	20.62	2.92	25.00
30	12.37	1.75	35.00
20	8.24	1.17	40.00
10	4.12	0.58	45.00
5	2.07	0.29	47.50
% TPC	**ED2003** (ml)	**Methacrylic Anhydride** (ml)	**Milli-Q** (ml)
50	21.83	1.68	25.00
30	13.10	1.01	35.00
20	8.73	0.67	40.00
10	4.37	0.34	45.00
5	2.18	0.17	47.50

Table A1.3: Material volumes required to produce Gelatin-ED2003-MAh by one-step synthesis with a total polymer content of 20%.

% Gelatin-MAh in TPC	**Gelatin** (g)	**ED2003** (ml)	**GMa** (ml)	**Milli-Q** (ml)
80	6.67	1.75	1.42	40
60	5.00	3.49	1.23	40
40	3.33	5.24	1.04	40
20	1.67	6.99	0.86	40

Table A1.4: Material volumes required to produce Gelatin-ED2003-GMa by one-step synthesis with a total polymer content of 20%.

% Gelatin-MAh in TPC	**Gelatin** (g)	**ED2003** (ml)	**GMa** (ml)	**Milli-Q** (ml)
80	6.67	1.65	1.51	40
60	5.00	3.30	1.43	40
40	3.33	4.95	1.34	40
20	1.67	6.60	1.25	40

Table A1.5: Material volumes required to produce Gelatin-ED2003-MAh by two-step synthesis with a total polymer content of 20%.

% Gelatin-MAh in TPC	**Gelatin** (g)	**MAh** (ml)	**Milli-Q** (ml)	**ED2003** (ml)	**MAh** (ml)	**Milli-Q** (ml)
80	6.67	1.28	20	1.75	0.13	20
60	5.00	0.96	20	3.49	0.27	20
40	3.33	0.64	20	5.24	0.40	20
20	1.67	0.32	20	6.99	0.54	20

Table A1.6: Material volumes required to produce Gelatin-ED2003-GMa by two-step synthesis with a total polymer content of 20%.

% Gelatin-GMa in TPC	**Gelatin** (g)	**GMa** (ml)	**Milli-Q** (ml)	**ED2003** (ml)	**GMa** (ml)	**Milli-Q** (ml)
80	6.67	1.28	20	1.65	0.23	20
60	5.00	0.96	20	3.30	0.47	20
40	3.33	0.64	20	4.95	0.70	20
20	1.67	0.32	20	6.60	0.93	20

Table A1.7: List of photoinitiators.

Photoinitiator	**Volume used per 50ml solution** (µl)	**%(w/v) per 10ml ethanol max absorption at 280nm** (%)	**Extinction coefficient** ($lmol^{-1}cm^{-1}$)
Irgacure 2959	300 µl	0.1000	2+
Irgacure 819	10 µl	0.1000	2+
Diphenyl (2,4,6-trimethylbenzoyl) phosphine oxide	300	0.0223	10
Thioxanthen-9-one	300	0.0016	6

2. Appendix 2 – Rheology Data

Table A2.1: Maximum Storage Modulus (G'_{max}) recorded after 20 minutes of curing for Gelatin-ED2003-MAh hydrogels produced using one-step synthesis.

% Gelatin-MAh in TPC	G'_{max} (kPa)	
100	13	±3
80	17	±4
60	21	±10
40	4	±1
20	4	±1
0	11	±1

Table A2.2: Maximum Storage Modulus (G'_{max}) recorded after 20 minutes of curing for Gelatin-ED2003-MAh hydrogels produced using two-step synthesis.

% Gelatin-MAh in TPC	G'_{max} (kPa)	
100	13	±3
80	153	±43
60	168	±27
40	13	±7
20	9	±0.5
0	11	±1

Table A2.3: Maximum Storage Modulus (G'_{max}) recorded after 20 minutes of curing for Gelatin-ED2003-GMa hydrogels produced using one-step synthesis.

% Gelatin-GMa in TPC	G'_{max} (kPa)	
100	91	±13
80	49	±2
60	63	±9
40	27	±2
20	15	±0.2
0	8	±0.4

Table A2.4: Maximum Storage Modulus (G'_{max}) recorded after 20 minutes of curing for Gelatin-ED2003-GMa hydrogels produced using two-step synthesis.

% Gelatin-GMa in TPC	**G'_{max}** (kPa)	
100	91	±13
80	60	±10
60	45	±4
40	47	±3
20	10	±0.1
0	8	±0.4

3. Appendix 3 – Compression Data

Table A3.1: Compressive stress at failure (σ_c), compressive strain at failure (ε_c), work of fracture (W_c), and elastic modulus (E_c)of gelatin-ED2003-MAh hydrogels produced by one-step synthesis with varying photoinitiators.

Photoinitiator	**σ_c**	**ε_c**	**W_c**	**E_c**
	(kPa)	(%)	(kJ/m^3)	(kPa)
Irgacure 2959	161 ±9	60 ±1	29 ±1	206 ±12
Irgacure 819	236 ±10	81 ±3	52 ±7	77 ±5
Dp246	1913 ±548	95 ±20	160 ±38	56 ±8
Tx91	296 ±41	92 ±9	35 ±8	0.1 ±0.01

Table A3.2: Compressive stress at failure (σ_c), compressive strain at failure (ε_c), work of fracture (W_c), and elastic modulus (E_c)of gelatin-ED2003-MAh hydrogels prepared by one-step synthesis.

% Gelatin-MAh in TPC	**σ_c**	**ε_c**	**W_c**	**E_c**
(%)	(kPa)	(%)	(kJ/m^3)	(kPa)
90	473 ±62	82 ±2	67 ±8	83 ±4
85	881 ±142	84 ±2	105 ±13	92 ±4
80	743 ±81	87 ±1	102 ±8	88 ±3
75	753 ±119	84 ±1	90 ±12	79 ±2
70	472 ±47	84 ±1	63 ±5	71 ±3
60	353 ±49	72 ±2	50 ±5	141 ±8
40	114 ±11	67 ±1	19 ±2	81 ±9
20	72 ±7	64 ±1	12 ±1	62 ±6

Table A3.3: Compressive stress at failure (σ_c), compressive strain at failure (ε_c), work of fracture (W_c), and elastic modulus (E_c)of gelatin-ED2003-MAh hydrogels prepared by two-step synthesis.

% Gelatin-MAh in TPC	**σ_c**	**ε_c**	**W_c**	**E_c**
(%)	(kPa)	(%)	(kJ/m^3)	(kPa)
100	407 ±26	79 ±1	59 ±3	98 ±6
95	320 ±59	75 ±1	46 ±6	94 ±5
90	2465 ±243	93 ±3	246 ±25	97 ±9
80	1882 ±308	95 ±3	201 ±27	77 ±5
70	203 ±42	77 ±2	24 ±4	37 ±2
60	175 ±47	77 ±3	22 ±4	36 ±3
0	27 ±3	69 ±2	6 ±0.52	36 ±5

Table A3.4: Compressive stress at failure (σ_c), compressive strain at failure (ε_c), work of fracture (W_c), and elastic modulus (E_c)of gelatin-ED2003-GMa hydrogels prepared by one-step synthesis.

% Gelatin-GMa in TPC	**σ_c**	**ε_c**	**W_c**	**E_c**
(%)	(kPa)	(%)	(kJ/m^3)	(kPa)
80	269 ±21	49 ±1	48 ±3	530 ±10
60	232 ±12	45 ±3	40 ±3	590 ±15
40	149 ±13	43 ±2	18 ±3	387 ±43
20	130 ±12	38 ±1	9 ±2	392 ±28

Table A3.5: Compressive stress at failure (σ_c), compressive strain at failure (ε_c), work of fracture (W_c), and elastic modulus (E_c)of gelatin-ED2003-GMa hydrogels prepared by two-step synthesis.

% Gelatin-GMa in TPC	**σ_c**	**ε_c**	**W_c**	**E_c**
(%)	(kPa)	(%)	(kJ/m^3)	(kPa)
100	238 **±21**	53 **±2**	46 **±3**	401 **±21**
80	221 **±15**	51 **±3**	39 **±3**	456 **±20**
60	202 **±25**	51 **±2**	34 **±4**	351 **±14**
40	118 **±17**	52 **±3**	19 **±2**	218 **±8**
20	34 **±7**	44 **±3**	5 **±1**	104 **±20**
0	20 **±6**	63 **±6**	4 **±1**	31 **±6**

4. Appendix 4 – Tensile Data

Table A4.1: Tensile stress at failure (σ_t), tensile strain at failure (ε_t), work of fracture (W_t), and elastic modulus (E_t) of gelatin-ED2003-MAh hydrogels prepared by one-step synthesis.

% Gelatin-MAh in TPC	σ_t	ε_t	W_t	E_t
(%)	(kPa)	(%)	(kJ/m^3)	(kPa)
90	14 ±2	125 ±11	9 ±2	11 ±1
80	11 ±2	82 ±4	5 ±1	14 ±2
70	16 ±2	107 ±6	9 ±1	17 ±3
60	15 ±2	123 ±10	9 ±2	12 ±1

Table A4.2: Tensile stress at failure (σ_t), tensile strain at failure (ε_t), work of fracture (W_t), and elastic modulus (E_t) of gelatin-ED2003-MAh hydrogels prepared by two-step synthesis.

% Gelatin-MAh in TPC	σ_t	ε_t	W_t	E_t
(%)	(kPa)	(%)	(kJ/m^3)	(kPa)
90	9 ±2	43 ±14	2 ±1	16 ±5
80	14 ±1	55 ±6	3 ±0.53	28 ±4
70	19 ±2	62 ±8	6 ±1	33 ±3
60	15 ±2	59 ±12	6 ±2	17 ±2

Table A4.3: Tensile stress at failure (σ_t), tensile strain at failure (ε_t), work of fracture (W_t), and elastic modulus (E_t) of gelatin-ED2003-GMa hydrogels prepared by one-step synthesis.

% Gelatin-GMa in TPC	σ_t	ε_t	W_t	E_t
(%)	(kPa)	(%)	(kJ/m^3)	(kPa)
90	9 ±0.55	74 ±6	3 ±0.43	15 ±1
80	13 ±2	78 ±13	3 ±0.51	30 ±4
70	42 ±8	66 ±9	13 ±4	60 ±6
60	31 ±4	57 ±6	8 ±1	56 ±5

Table A4.4: Tensile stress at failure (σ_t), tensile strain at failure (ε_t), work of fracture (W_t), and elastic modulus (E_t) of gelatin-ED2003-GMa hydrogels prepared by two-step synthesis.

% Gelatin-GMa in TPC	**σ_t**	**ε_t**	**W_t**	**E_t**
(%)	(kPa)	(%)	(kJ/m^3)	(kPa)
90	23 ±3	50 ±6	6 ±1	53 ±3
80	21 ±3	69 ±8	7 ±2	33 ±3
70	43 ±5	93 ±8	19 ±3	42 ±2
60	28 ±3	58 ±9	6 ±0.44	53 ±3

5. Appendix 5 – NMR Spectra

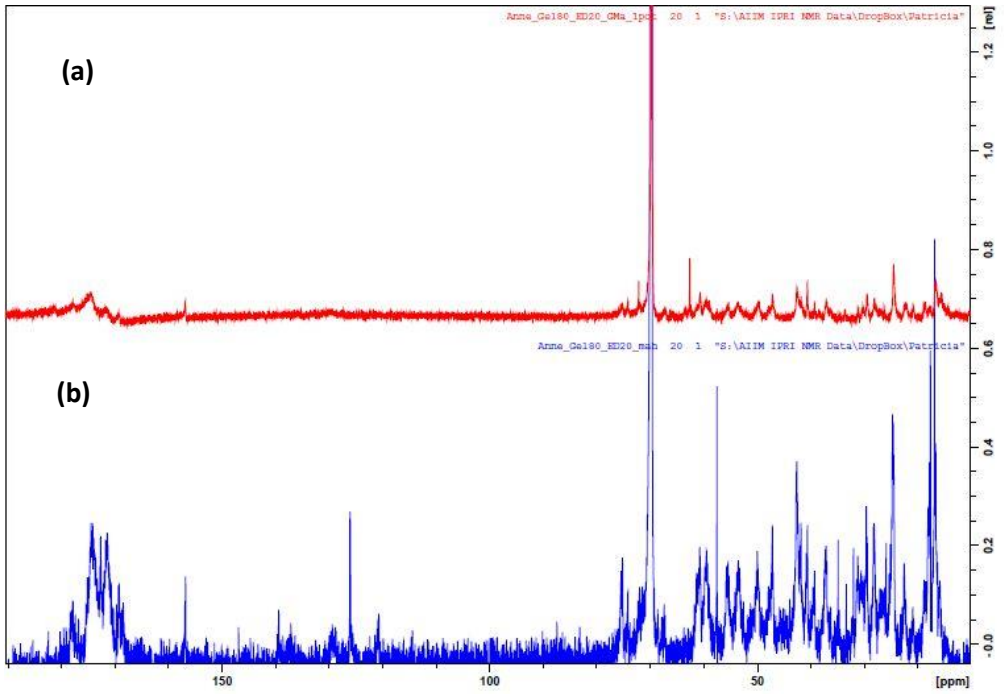

Figure A5.1: ^{13}C NMR Spectra for (a) G(80%):E(20%) GMa, with a TPC of 20% and produced using the one-step synthesis method and (b) G(80%):E(20%) methacrylated using MAh, with a TPC of 20% and produced using the one-step synthesis method.

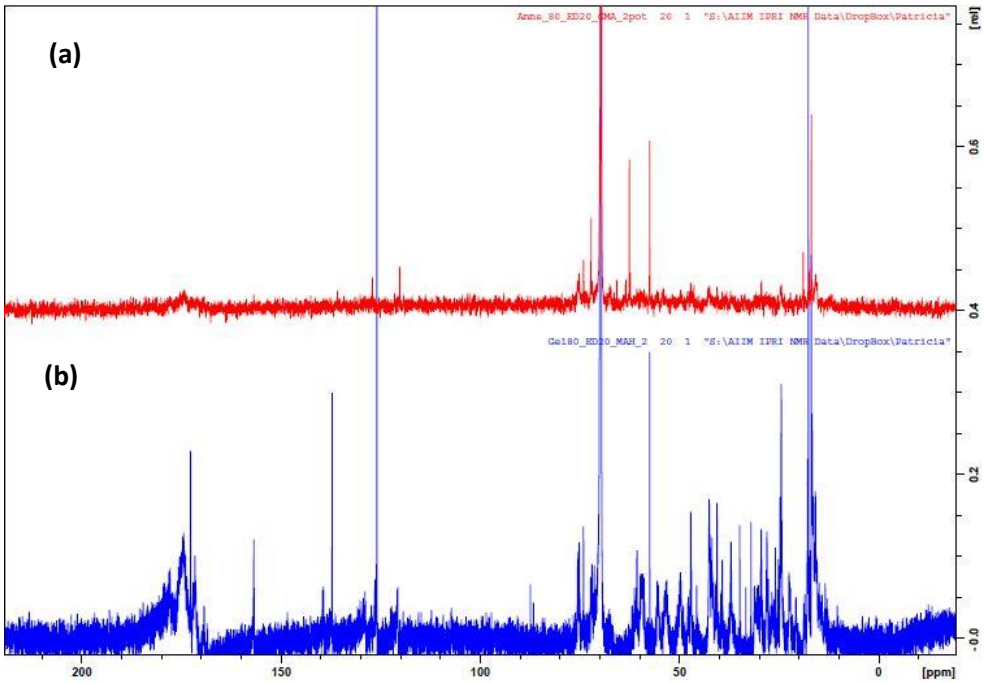

Figure A5.2: ^{13}C NMR Spectra for (a) G(80%):E(20%) GMa, with a TPC of 20% and produced using the two-step synthesis method and (b) G(80%):E(20%) MAh, with a TPC of 20% and produced using the two-step synthesis method.

6. Appendix 6 – FTIR Spectra

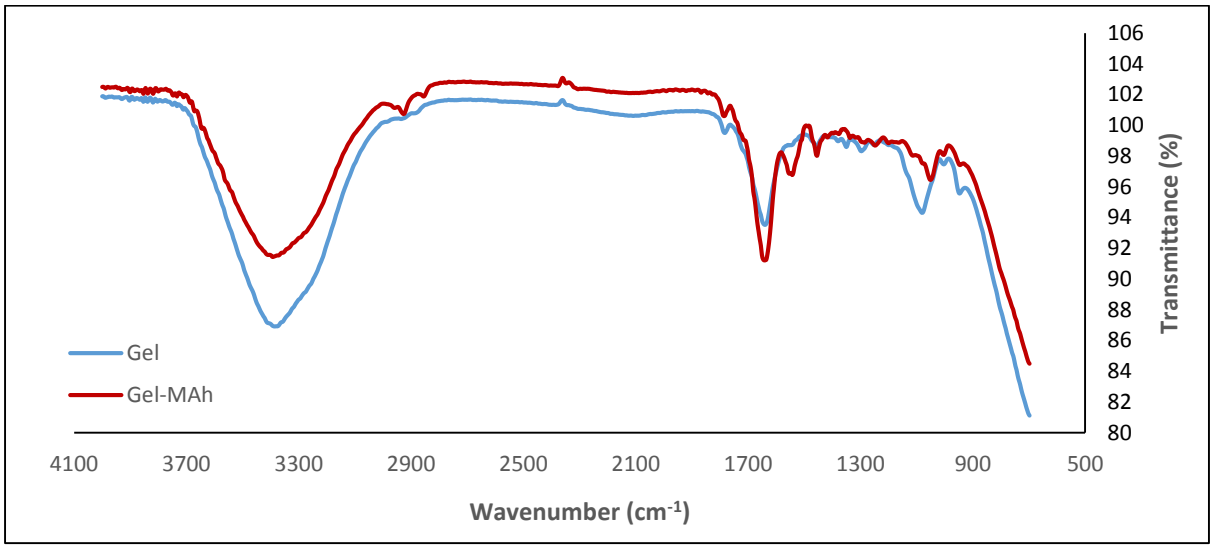

Figure A6.1: FTIR Spectre for Gelatin and Gel-MAh, with a TPC of 20%.

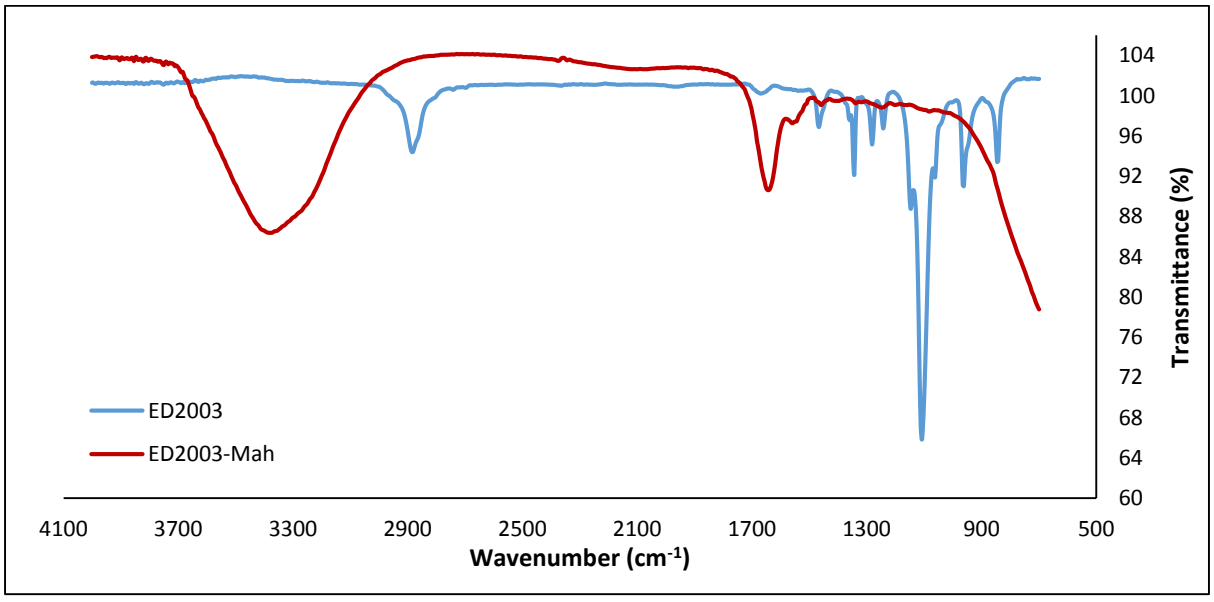

Figure A6.2: FTIR Spectre for ED2003 and ED2003-MAh, with a TPC of 20%.

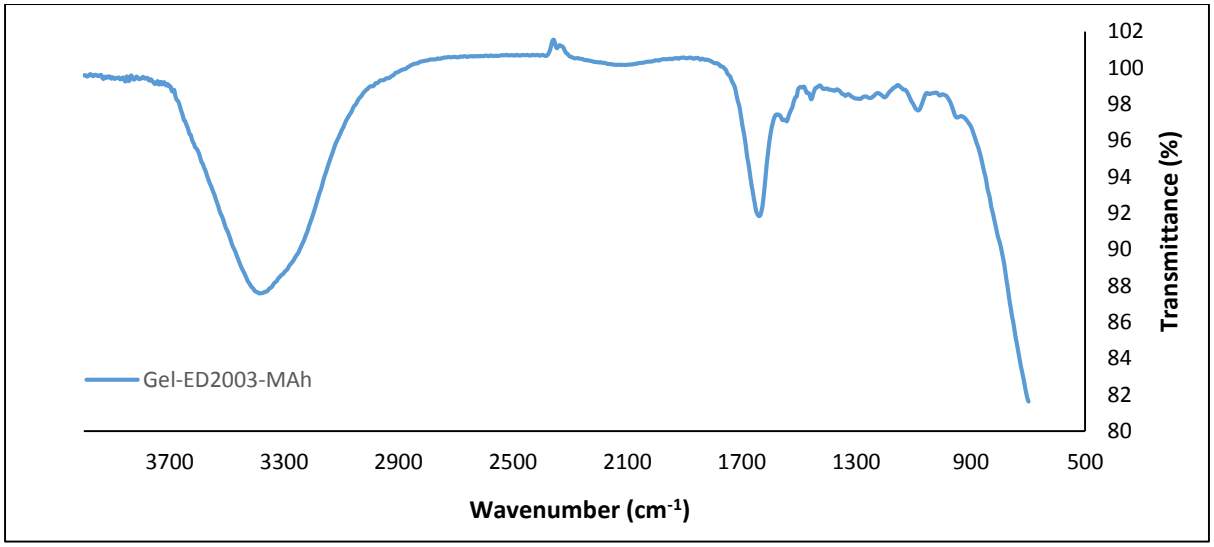

Figure A6.3: FTIR Spectre for G(80%):E(20%) methacrylated using MAh, with a TPC of 20% and produced using the one-step synthesis method.